PUBLICATIONS OF THE ASTRONOMICAL SOCIETY OF THE PACIFIC
100: 427–451, April 1988

BASIC ELEMENTS OF THE THEORY OF ACCRETION*

A. TREVES AND L. MARASCHI
Dipartimento di Fisica dell'Università di Milano, Italy
AND
M. ABRAMOWICZ
Scuola Internazionale Superiore di Studi Avanzati, Trieste, Italy

Received 1988 January 8

ABSTRACT

The paper reviews what we consider to be the essential aspects of the theory of accretion. A general overview is given in Section I. The treatments of accretion of cold gas onto a moving star by Hoyle and Lyttleton and of spherical adiabatic accretion by Bondi are summarized in Section II. The formation of spectra in accretion flows onto neutron stars and white dwarfs is described in Section III, with brief mention of the effects of a magnetic field anchored to the star. Spherical accretion onto black holes is treated in Section IV; in particular we underline the differences between classes of models leading to different efficiencies and spectra. We stress the role of a magnetic field entangled in the infalling plasma and the importance of the Comptonization process. The effects of radiation pressure in spherical accretion are then discussed.

Thin accretion disks in the standard α approximation are introduced in Section V. The stability conditions for thermal and viscous processes are examined and the bivalued region of the $\Sigma, \dot{\mathfrak{M}}$ plot is discussed in view of a possible limit cycle behavior. Thick disks and their stability are briefly treated in Section VI.

Section VII offers threads between theory and observations mentioning the astrophysical systems where accretion plays a major role (cataclysmic variables, X-ray binaries, Active Galactic Nuclei) pointing out successes and weaknesses of the present models.

Key words: mass accretion–mass exchange–circumstellar disks

I. Introduction

Accretion is the process by which a gravitating body aggregates matter from its surroundings. Its importance was first recognized in connection with the physics of the solar system (formation of planets). A few years later Hoyle and Lyttleton (1939) examined the possible change in luminosity of a Sun-like star due to its passage through an interstellar gas cloud, with a view to explaining the Earth's climatic variations. This fundamental paper contains the first derivation of the accretion rate for a star moving through cold gas.

The next important step in the development of accretion theory was the paper by Bondi (1952), who considered the infall of gas described by a polytropic equation of state onto a static gravitating body. The accretion rate was calculated and a full analytic solution for the fluid flow was given. The equations formulated by Bondi are also relevant for the case of outflow, i.e., for the theory of stellar (or solar) winds which, from the late fifties, were the subject of an enormous amount of research (e.g., Parker 1963; Holzer and Axford 1970).

Renewed interest for accretion was related in the sixties to two fundamental astrophysical discoveries: quasi-stellar radio sources (quasars) with extremely large luminosities ($L \sim 10^{12}\ L_\odot$) produced in comparatively small regions ($r \sim 1$ pc) and X-ray sources, with large powers emitted predominantly at very high temperatures ($\sim 10^7$ K). Salpeter (1964) and Zel'dovich (1964) were the first to examine the possibility of producing the luminosity of quasars by accretion of matter onto a collapsed object of large mass, which must necessarily be a black hole (though the word black hole was not yet in use when these papers were written). Shklovsky (1967) was the first to propose that a bright galactic X-ray source (Scorpius X-1) could be a binary system containing a neutron star accreting mass from its companion.

It was immediately apparent that, in more quantitative studies, the boundary conditions both at large distances from the collapsed object and at its surface would play an essential role. If the accreting matter possesses angular momentum, this has to be removed before the matter can

*One in a series of invited review articles currently appearing in these *Publications*.

fall. The simplest situation in this respect is that of a disk in which matter slowly spirals inward, as viscosity between differentially rotating rings transports angular momentum outward. The role of an accretion disk in binary X-ray sources and the similarity with the cataclysmic variables were pointed out by Prendergast and Burbidge (1968). The importance of disk accretion around a massive black hole was recognized by Lynden-Bell (1969), with special reference to the center of our Galaxy. Shakura (1972), Pringle and Rees (1972), and Shakura and Sunyaev (1973) gave a detailed discussion of the accretion disk with a computation of the emission spectrum. Disk accretion has the important characteristic that the properties of the disk itself are largely independent of the nature of the central object, except at the inner boundary. In order to reach this inner boundary a fixed fraction (50%) of the potential energy gained by the gas in approaching the gravitating body must be radiated away, thus fixing the efficiency of the process.

The effect of the inner boundary conditions is the following: if the central object is a white dwarf or a neutron star, the accreting gas must be slowed down and brought to rest at the surface of the star. Again the efficiency of the process is fixed and the mechanisms by which the slowing down occurs determine the emitted spectrum.

The presence of a strong surface magnetic field on a neutron star (10^9–10^{12} G) or a white dwarf (10^7 G) introduces a further feature into the models. It defines a region (magnetosphere) where the accretion flow is dominated by magnetic pressure. Thus, even if an accretion disk may be present outside this region, within it the flow will be quasi-radial along the field lines. Obviously the radiation processes are strongly affected.

The case of accretion onto a black hole at first sight seems simpler. Two alternative approximations can be adopted: either a disk, which extends to the innermost stable orbit, or a spherically symmetric flow. In the former case the efficiency is fixed, as mentioned above, while in the second case it is the main unknown of the problem.

For spherical accretion onto black holes, the efficiency of conversion of gravitational potential energy into radiation is extremely small, if the accretion rate is low (Shapiro 1973*a*), but it may be substantially enhanced if the accreting plasma is even weakly magnetized, leading to internal heating by dissipative processes as proposed by Shvartsman (1971) and Meszaros (1975). Here and in the following the efficiency η is defined by $\eta \equiv L/\dot{\mathfrak{M}}c^2$.

Profound changes in the accretion flows summarized above are introduced when the accretion luminosity becomes close to the Eddington luminosity for which radiation pressure balances gravity (see eq (4.10))

$$L_E = \frac{4\pi G \mathfrak{M} m_p c}{\sigma_T} \quad . \tag{1.1}$$

This is also called the critical luminosity and, associated with it, there is a critical accretion rate

$$\dot{\mathfrak{M}}_{crit} = L_E/c^2 = \frac{4\pi G \mathfrak{M} m_p}{c\sigma_T} \quad . \tag{1.2}$$

In the case of white dwarfs and neutron stars no stationary solution exists if the accretion rate is larger than $\dot{\mathfrak{M}}_{crit}/\eta$, while in the case of a black hole the radiation efficiency η can be reduced so that the hole is able to swallow mass at an arbitrarily high rate with a limited energy output. The evolution of accretion theory is sketched in Figure 1.

The aim of this review is to present the basic elements of the theory of accretion in a simple and unified way. We will concentrate on results of general interest without going into the fine details of specific astrophysical models, but merely indicating which systems may be described by a certain class of accretion models. A special effort is made to explain in elementary terms the spectra deriving from different choices in the description of the accretion flow.

The plan of the paper is the following: in Section II, approximate formulae for the accretion rate are obtained through elementary considerations; next the theory of spherical accretion of a polytropic gas is introduced. The effects of the termination of the flow at the surface of a neutron star or white dwarf are discussed in Section III, where the interaction with a magnetic field anchored to the star is also examined. In Section IV, spherical accretion onto black holes is described considering, in particular, the role of the magnetic field in the accreting plasma and the issue of radiation pressure. Disk accretion is discussed in Section V, and the basic ideas of thick accretion disks are presented in Section VI. Section VII introduces the relations between the theoretical models and the observational world. Some concluding remarks are given in Section VIII. A summary of most-frequently-used symbols is reported in Table I.

Some of the subjects treated in this paper can be found

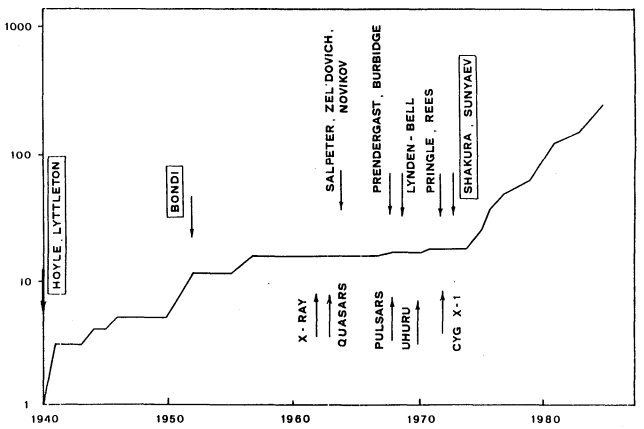

FIG. 1–Number of authors who published, prior to a given date, articles in the *Monthly Notices of the Royal Astronomical Society*. The basic papers and observational discoveries are marked with arrows (from Abramowicz and Marsi 1987).

TABLE I

LIST OF THE PRINCIPAL SYMBOLS USED IN THE PAPER

B = magnetic field
D = height of shock
F = radiation flux from surface
f = radial function defined in 5.12
H = half thickness of the disk
L_E = Eddington luminosity
l = specific angular momentum
$\mathfrak{M}$ = mass of the accreting body
$\dot{\mathfrak{M}}$ = accretion rate
$\dot{\mathfrak{M}}_c$ = critical accretion rate
P = pressure
Q^+ = viscous heat production rate
Q^- = viscous heat loss
q = horizontal heat flux
R_{in} = inner edge of the disk
r_A = Alfven radius
r_c = accretion radius
r_s = sonic radius
r_{st} = star radius
r_G = gravitational radius
r_{tr} = trapping radius
T_{eff} = effective temperature
T_s = shock temperature
V_s = sound velocity
V_k = Keplerian velocity
V_R = radial velocity in the disk
V_φ = azimuthal velocity
W_B = magnetic energy density
W_G = gravitational energy density
α = viscosity parameter
β = ratio of gas pressure to total pressure
γ = polytropic index
Γ = specific heating rate
κ = opacity coefficient
η = radiation efficiency
Λ = specific cooling rate
μ = mean molecular weight
ν = kinematic viscosity
ρ = density
Σ = surface density of the disk
τ_T = Thomson optical depth

in textbooks such as *Relativistic Astrophysics* by Zel'dovich and Novikov (1971) and *Black Holes, White Dwarfs, and Neutron Stars* by Shapiro and Teukolsky (1983). A more extended and detailed account of the fundamentals of accretion theory in astronomy can be found in the recently published volume *Accretion Power in Astrophysics* by Frank, King, and Raine (1985).

II. Basics of Accretion

A. *Accretion of a Cold Gas*

Consider a star of mass $\mathfrak{M}$ moving with velocity v_∞ in a cold gas of density ρ_∞ (Hoyle and Lyttleton 1939). In the rest frame of the star at large distance the gas streams with a uniform velocity $-v_\infty$. The cold particles constituting the gas will follow Keplerian orbits in the gravitational field. They are deflected on the rear side of the object and particles with a given impact parameter intersect the star trajectory at a certain distance r from the star. Suppose that at r_c they collide with the particles having the symmetric trajectory and that through the collisions the transverse momentum can be dissipated. If the remaining parallel velocity component is lower than the escape velocity from the star at r the particles will be gravitationally captured. Using Newtonian mechanics one can calculate that, with the above hypothesis, capture occurs for impact parameters smaller than

$$r_c = 2G\mathfrak{M}/v_\infty^2 \ . \tag{2.1a}$$

Correspondingly, the accretion rate is given by

$$\dot{\mathfrak{M}} = \rho_\infty v_\infty \pi r_c^2 = 4\pi\rho_\infty G^2\mathfrak{M}^2/v_\infty^3 \ . \tag{2.1b}$$

The two formulae (2.1a and 2.1b) play a fundamental role in the theory of accretion.

Consider now the other limit of a star at rest in a fluid of temperature T (Bondi 1952). The influence of the gravitational field will be strong in the region where the sound speed $v_{s\infty} = (\partial p/\partial\rho)_\infty^{1/2}$, is smaller than the escape velocity, i.e., for

$$r < r_c = 2G\mathfrak{M}/v_{s\infty}^2 \ . \tag{2.2}$$

Therefore, the critical radius for accretion is formally similar to that of the previous problem, provided the sound velocity is used instead of the bulk velocity of the cold fluid. The accretion rate will be roughly given by

$$\dot{\mathfrak{M}} = 4\pi r_c^2 \rho v_{s\infty} = 4\pi\rho_\infty G^2\mathfrak{M}^2/v_{s\infty}^3 \ . \tag{2.3}$$

In the general case of a star moving with velocity v in a fluid where the sound speed is v_s, it can be argued that the

accretion rate should be given by

$$\dot{\mathfrak{M}} \simeq \frac{4\pi(G\mathfrak{M})^2}{(v_\infty^2 + v_{s\infty}^2)^{3/2}} , \tag{2.4}$$

which reduces to equations (2.1) and (2.3) for $v_s = 0$ and $v_\infty = 0$, respectively.

B. *Spherical Accretion: Bondi Theory*

A rigorous treatment of the flow dynamics around a Newtonian point mass, taking into account pressure forces, was given by Bondi in 1952. The simplest formulation of the stationary spherical problem is specified by the equations

$$\dot{\mathfrak{M}} = 4\pi r^2 v \qquad \text{mass conservation} , \tag{2.5}$$

$$v\frac{dv}{dr} = -\frac{1}{\rho}\frac{dp}{dr} - \frac{G\mathfrak{M}}{r^2} \qquad \text{Euler equation} , \tag{2.6}$$

and

$$P = P(\rho) \qquad \text{equation of state} . \tag{2.7}$$

Bondi considered a polytropic equation of state

$$P \propto \rho^\gamma \tag{2.8}$$

with

$$1 \leq \gamma \leq 5/3 .$$

If we introduce the local sound velocity, the equations reduce to the form

$$\frac{v^2}{2} + \frac{1}{\gamma - 1}v_s^2 - \frac{G\mathfrak{M}}{v} = B \tag{2.9}$$

$$v = \frac{\dot{\mathfrak{M}}}{4\pi\rho_\infty r^2}\left(\frac{v_{s\infty}}{v_s}\right)^{\frac{2}{\gamma-1}} , \tag{2.10}$$

where B is an integration constant and ∞ labels quantities at large distance with respect to r_c (eq. (2.2)).

The first equation represents an ellipse and the second a hyperbola in the v, v_s plane. The two points of intersection correspond to the existence of two solutions, one subsonic and one supersonic (see Zel'dovich and Novikov 1971). They have been studied in detail by Bondi (see also Frank *et al.* 1985). Here we consider only those where the velocity at infinity tends to zero, excluding the cases of outflows which are relevant for stellar winds. The condition implies that the constant B in equation (2.9) equals $(1/\gamma - 1)v_{s\infty}^2$. Moreover, we suppose that the velocity increases monotonically toward the central star, which corresponds to the case of maximal accretion rate. In this case a sonic point is present at

$$r_s = \frac{1}{4}(5 - 3\gamma)\frac{G\mathfrak{M}}{v_{s\infty}^2} , \tag{2.11}$$

and the accretion rate is uniquely determined by the equation

$$\dot{\mathfrak{M}} = \pi G^2 \mathfrak{M}^2 \frac{\rho_\infty}{v_{s\infty}^3}\left[\frac{2}{5 - 3\gamma}\right]^{\frac{5-3\gamma}{2\gamma-1}} . \tag{2.12}$$

This expression for $\dot{\mathfrak{M}}$ differs from that obtained from elementary considerations (eq. (2.3)) only by a small numerical factor. Within the sonic radius the fluid falls essentially freely.

Particularly interesting is the explicit form of the solution in the case $\gamma = 5/3$ (nonrelativistic monoatomic gas). From equation (2.12) the accretion rate is given by

$$\dot{\mathfrak{M}} = \pi \frac{(G\mathfrak{M})^2}{v_{s\infty}^3}\rho_\infty . \tag{2.13}$$

The sonic point is at $r = 0$, therefore the solution is everywhere subsonic. For $r \ll r_c = G\mathfrak{M}/v_{s\infty}^2$, the velocity is

$$v = \frac{1}{\sqrt{2}}\left(\frac{G\mathfrak{M}}{r}\right)^{1/2} , \tag{2.14}$$

i.e., one-half of the free-fall velocity, and the density and pressure are

$$\rho = \rho_\infty\left(\frac{2r}{r_c}\right)^{-3/2} , \tag{2.15}$$

$$P = P_\infty\left(\frac{2r}{r_c}\right)^{-5/2} . \tag{2.16}$$

The temperature T can be expressed as p/nk, where n is the particle density, i.e., $T = p\mu m_p/k\rho$, where μ is the mean molecular weight. For ionized hydrogen $\mu = 1/2$, and

$$T = \frac{3}{20}\frac{m_p}{k}\frac{G\mathfrak{M}}{r} . \tag{2.17}$$

Note that the temperature in this limiting case does not depend on the boundary conditions.

III. Spherical Accretion onto White Dwarfs and Neutron Stars

In the spherical adiabatic approximation the accretion flow onto a compact star (neutron star or white dwarf) can be described by the solutions discussed in the previous section up to some distance from the star. The infall of the plasma is halted at the surface of the star and the solutions must be matched with appropriate boundary conditions. Since practically all the energy release occurs at this boundary, the microscopic processes by which the particles are decelerated determine the radiation spectrum.

Two extreme approximations are possible. In the first the energy loss of protons occurs through Coulomb collisions in the atmosphere of the star which requires, for a proton incident on a neutron star, a depth of 2–30 g cm^{-2} (the kinetic energy of the proton is $\sim$ 100 MeV). The

energy is uniformly dissipated and thermalized in this thick layer, which radiates roughly as a blackbody. The associated temperature is

$$T_{\rm eff} = (L/\sigma 4\pi r_{\rm st}^2)^{1/4} , \qquad (3.1)$$

which is the minimum temperature at which the radiation can emerge.

At the other extreme, if the proton momenta are randomized in a time much shorter than the time scale for energy loss, the transition from the supersonic flow to the settling atmosphere occurs through a strong adiabatic shock discontinuity. The temperature below the shock is then

$$T_s = \frac{3}{8}\frac{G\mathfrak{M}m_p}{kr_{\rm st}} , \qquad (3.2)$$

which is the maximum temperature at which radiation can be emitted. For a typical neutron star $T_{\rm eff} = 1 \times 10^7 (L_{37})^{1/4}$ K and $T_s = 10^{12}$ K, while for a typical white dwarf $T_{\rm eff} = 6 \times 10^5 (L_{37})^{1/4}$ K and $T_s = 10^9$ K, where L_{37} is the luminosity in units of 10^{37} erg s^{-1}.

More realistic calculations along the first line of approach were first carried out in the case of a neutron star by Zel'dovich and Shakura (1969) and further expanded by Alme and Wilson (1973). It is found that a large fraction of the power is emitted as blackbody radiation from the inner layers of the atmosphere; however, the upper layers are heated to higher temperatures and cool off mainly through inverse Compton scattering with the outgoing blackbody photons. This produces a high-energy tail on the blackbody distribution, which increases in importance with decreasing accretion rate (see Fig. 2).

The second type of approximation has been treated in detail in the case of a neutron star by Shapiro and Salpeter (1975). The adiabatic shock hypothesis requires very efficient plasma instabilities, so that protons are randomized in a time comparable to the inverse of the plasma frequency rather than to the inverse of the Coulomb collision frequency. This is a rather extreme assumption since, in the case of a neutron star, the ratio between the two frequencies is of the order of 10^{12}. The extent of the hot emission zone below the shock is determined by the time required for the ions to transfer all their energy to the electrons, which cool rapidly via Compton scattering of the photons. The computed spectra show a blackbody component analogous to that computed by Zel'dovich and Shakura (1969); however, a large fraction of the total power is emitted in a high-energy component, which extends to the MeV region, due to Comptonization by relativistic electrons (see Section IV) immediately behind the shock (see Fig. 3).

On a white dwarf the incident protons are much less energetic (100 keV). Therefore, the depth in which their energy is deposited is much smaller and the shock approximation is usually adopted (Hoshi 1973; Aizu 1973). A particularly simple description is given by Fabian, Pringle, and Rees (1976). The layer below the shock (which, for reasonable values of the parameters, turns out to be smaller than the radius of the star) is assumed to be isothermal and homogeneous. The temperature and density are assumed to have the postshock values. The height of the shock D is determined by the condition that the emissivity of the shocked gas is sufficient to radiate the deposited power. If the emission mechanism is bremsstrahlung, the height D is given by the simple expression

$$D = 3 \times 10^7 \dot{\mathfrak{M}}_{20} R_9^{1/2} \quad \text{cm} , \qquad (3.3)$$

where $\dot{\mathfrak{M}}_{20}$ is the accretion rate in units of 10^{20} g s^{-1} and R_9 is the white-dwarf radius in units of 10^9 cm. Note that the shock height increases with decreasing accretion rate. Inserting the same scaling, the temperature, as from equation (3.1), is given approximately by

$$T_s = 3.7 \times 10^8 (\mathfrak{M}/\mathfrak{M}_\odot) R_9^{-1} K . \qquad (3.4)$$

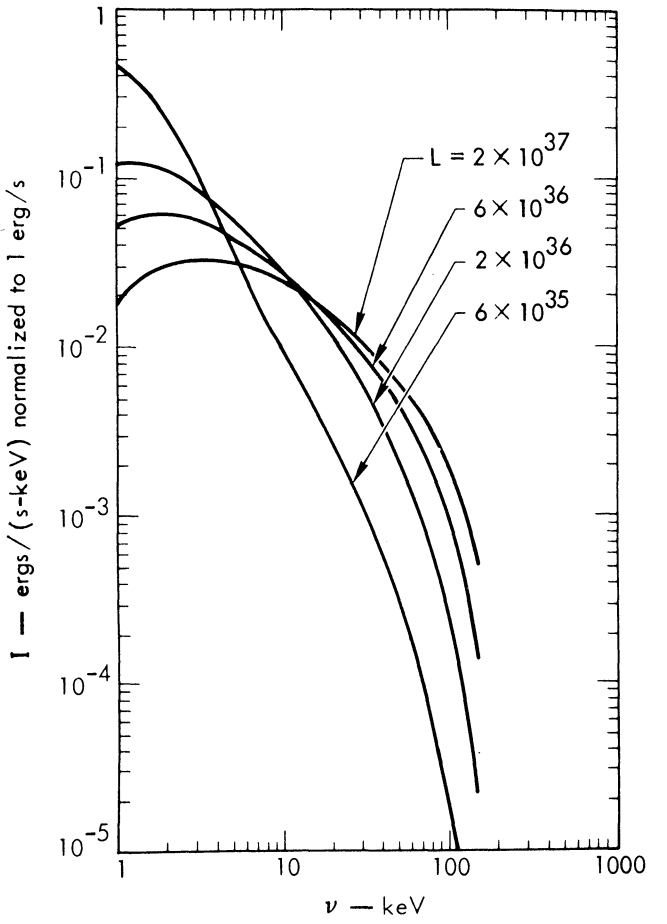

FIG. 2–X-ray spectra from accretion of a nonmagnetized neutron star of 0.5 $\mathfrak{M}_\odot$, in the hypothesis of no shock formation (from Alme and Wilson 1973).

Accretion on Stars Endowed with a Magnetic Field

Neutron stars and white dwarfs may have large magnetic fields. On neutron stars typical values of the surface

ACCRETION ONTO NEUTRON STARS

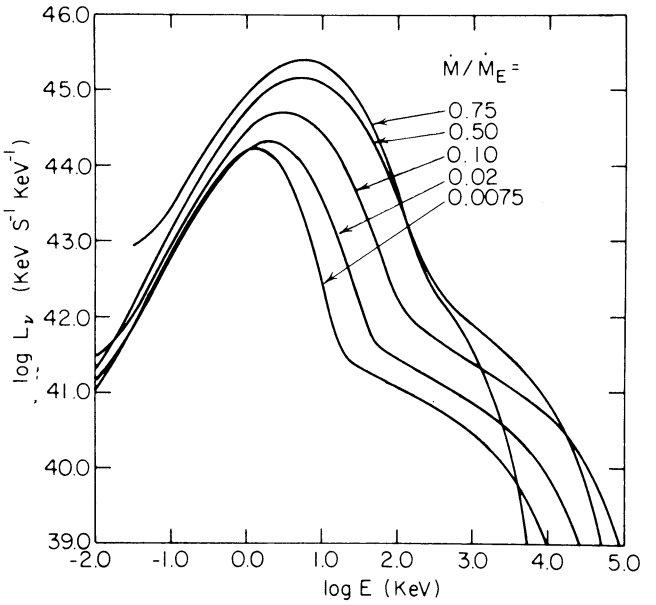

FIG. 3–Spectra from a 1.1 $\mathfrak{M}_\odot$ unmagnetized neutron star with shock formation (from Shapiro and Salpeter 1975).

field, $B_0 = 10^{12}$ G, are indicated by various estimates; on white dwarfs the surface field can reach 10^7–10^8 G. Fields of this size affect the dynamics of accretion. The radius at which the influence of the field becomes important can be evaluated by equating the ram pressure of the infalling plasma W_G to the magnetic pressure W_B. For spherical accretion

$$W_G = \frac{\dot{\mathfrak{M}}(G\mathfrak{M})^{1/2}}{4\pi\sqrt{2}} r^{-5/2} , \tag{3.5}$$

and for a dipolar field

$$W_B = \frac{B_0^2}{8\pi}\left(\frac{r}{r_{st}}\right)^{-6} , \tag{3.6}$$

where r_{st} is the star radius.

The radius at which $W_G = W_B$, usually called the Alfven radius, is given by Davidson and Ostriker (1973), Lamb, Pethick, and Pines (1973), and Baan and Treves (1973) as

$$r_A = \left(\frac{B_0^2 r_{st}^6}{\sqrt{2G\mathfrak{M}\dot{\mathfrak{M}}}}\right)^{2/7} . \tag{3.7}$$

For a neutron star with an accretion luminosity $L \sim 10^{37}$ erg s^{-1}, a typical value for a binary X-ray source, $r_A = 3 \times 10^8$ cm. Therefore, in a large volume around the neutron star accretion is dominated by the magnetic field. In the case of white dwarfs the Alfven radius turns out to be comparable to the white-dwarf radius.

Within the Alfven radius the accreting material is supposed to follow the magnetic-field lines. The magnetic surface, identified by the condition that its equatorial radius equals the Alfven radius, defines the path of the accretion flow. For a dipole field its shape resembles two funnels centered on the magnetic poles. Hence, the accreting material is channeled onto small areas around the polar caps. Elementary considerations yield for the radius of the polar cap the approximate formula

$$r_{pc} = r_{st}\left(\frac{r_{st}}{r_A}\right)^{1/2} . \tag{3.8}$$

Considering again a neutron star with a luminosity of 10^{37} erg s^{-1}, one has that a fraction $f = (r_{st}/r_{pc})^2 \simeq 1\%$ of the star surface is hit by the accreting matter. The blackbody temperature evaluated by equation (3.1) is therefore raised by a factor 3, if energy transfer by conduction is neglected.

For the description of the accretion columns, the spherical approximation is still relevant, though limited to a fraction f of the solid angle. For a neutron star with a high magnetic field the radiative processes are strongly dominated by cyclotron radiation in the semirelativistic regime kT = 10–100 keV. The radiative transfer of the cyclotron radiation in the magnetic funnel is enormously complicated due to the anisotropy of emission and absorption processes and is much beyond the scope of this review. Suffice it to say that, while the general properties of accretion columns on white dwarfs seem recently understood (e.g., Lamb 1985), those of neutron-star accretion columns still present unsolved problems, a basic one being whether the outgoing radiation is beamed along the column or in a wide-angle hollow cone (see, however, Meszaros and Nagel 1985*a*,*b*).

IV. Spherical Accretion onto Black Holes

It seems well established that the collapse of stars larger than a few solar masses would proceed through the Schwarzschild event horizon $r_G = 2G\mathfrak{M}/c^2$, giving rise to a black hole. The properties of the Schwarzschild metric are such that no radiation emitted below the horizon can reach the observer at infinity. Hence, if matter falling into a black hole releases its energy entirely within the horizon, the efficiency $\eta = L/\dot{\mathfrak{M}}c^2$ of the process for the external observer may be zero. However, in any realistic description of the accreting plasma, some fraction of the kinetic (gravitational) energy is radiated away before reaching the gravitational radius r_G. The computation of this fraction is one of the main issues in the problem of spherical black-hole accretion. It is clear that the most important region in this respect is just outside r_G, where $v \simeq c$; thus special and general relativistic corrections should be taken into account.

In the simplest, adiabatic, Newtonian approximation the expected temperature at r_G is $T \simeq 10^{12}$ K, as given by

equation (2.17). This is independent of the mass of the black hole.

Shapiro (1973*a*) solved under specific hypotheses a full set of relativistic equations, coupling the dynamical and thermodynamical behavior of the accreting plasma. This consists of adding to the dynamic equations (2.5, 2.6), rewritten in the fully relativistic form, the energy balance equation (e.g., Shvartsman 1971)

$$v\left(\frac{d\epsilon}{dr} - \frac{\epsilon+P}{n}\frac{dn}{dr}\right) = \Lambda - \Gamma \ , \tag{4.1}$$

where v is the velocity, n is the scalar number density, ϵ is the proper internal-energy density, P is the pressure, and Λ and Γ are the specific cooling and heating rates in erg $cm^{-3}\ s^{-1}$.

Shapiro (1973*a*) considered the case of $\Gamma = 0$ and bremsstrahlung as a cooling mechanism; he found that a solar-mass black hole accreting the interstellar medium radiates with an efficiency $\eta \simeq 10^{-10}$–10^{-9}. The efficiency increases for large accretion rates, since it is roughly proportional to the square of the density of the flow. However, it remains rather low $\eta \leq 10^{-4}$, with the equal sign corresponding to the critical accretion rate $\dot{\mathfrak{M}} \sim \dot{\mathfrak{M}}_c$. The radial dependence of the velocity closely approaches the free-fall case.

Subsequently, on the basis of this result, several authors, interested mainly in the computation of the emitted spectrum, have simply assumed velocity and density profiles similar to the free-fall case and have devoted attention to the energy-balance equation (4.1) only.

In a Newtonian scheme, if one supposes that the infall velocity scales as the free-fall velocity $v \propto r^{-1/2}$, and for the case of a completely ionized nonrelativistic hydrogen plasma, equation (4.1) reduces to the form (Meszaros 1975)

$$\frac{dT}{dr} = -\frac{T}{r} + \frac{4\pi m_p r^2(\Lambda - \Gamma)}{3k\dot{\mathfrak{M}}} \ . \tag{4.2}$$

This is a single equation for T and can be solved analytically or numerically if the heating and cooling rates are specified. The outgoing spectrum and luminosity can be computed, in the case of a transparent atmosphere, by integrating the spectral emissivities over the accreting volume.

A. *Role of the Magnetic Field in the Accreting Plasma*

Shvartsman (1971) pointed out that, if the infalling plasma is even weakly magnetized, the accretion process will amplify the field B. In fact, from the conservation of magnetic flux which is valid for highly conducting flows, it follows that the radial component of B should increase as r^{-2} and the magnetic energy density W_B as r^{-4}. The buildup of the magnetic energy density occurs through the gravitational field, which is responsible for the compression of the plasma. Since the gravitational energy density W_G scales as $r^{-5/2}$ (eq. (3.5)) at sufficiently small radii the magnetic energy density approaches the gravitational one. On energetic and stability grounds it is assumed that at small enough radii $W_G \simeq W_B$, giving

$$B = \dot{\mathfrak{M}}^{1/2} G\mathfrak{M}^{1/4} r^{-5/4} \ , \tag{4.3}$$

independent of the initial value of B. For critical accretion rates equation (4.3) gives, at $r = r_G$, $B = 5 \times 10^7$ G for a 10 $\mathfrak{M}_\odot$ black hole and $B = 10^4$ G for 10^8 $\mathfrak{M}_\odot$. Alternative configurations are possible if one considers an initially ordered rather than chaotic magnetic field (see, e.g., Bisnovatyi-Kogan 1979).

Shapiro (1973*b*) showed that the dynamical effect of the B field is small, as it does not impede the radial flow. However, the field has two main consequences. The most obvious is the activation of cyclotron (synchrotron) radiation from the thermal electrons as an emission process (cooling mechanism). The inclusion of this effect leads to radiative efficiencies far exceeding those obtained in the case when only bremsstrahlung is considered (Shapiro 1973*a*). Moreover, it shifts the frequency at which maximum emission occurs from values of the order of kT = 1–10 MeV, appropriate for bremsstrahlung, to the thermal synchrotron frequency

$$\nu_s = \frac{3}{4}\frac{eB}{\pi mc}\left(\frac{kT}{mc^2}\right)^2 \ , \tag{4.4}$$

which falls in the far-infrared region of the spectrum.

A more subtle effect, which was clearly recognized by Meszaros (1975), is that the equipartition assumption implies a complicated physical situation, with instabilities and field reconnection preventing excessive growth of W_B and leading to turbulent motion. A certain amount of dissipation must be associated with these processes, which is equivalent to saying that some fraction of the gravitational energy is transformed into heat, giving rise to a heating term Γ in equations (4.1, 4.2). With this assumption Γ can be written as a fraction of the gravitational energy density divided by the infall time, i.e.,

$$\Gamma \simeq \frac{1}{8\pi}\frac{G\mathfrak{M}\dot{\mathfrak{M}}}{r^4} \ . \tag{4.5}$$

Equation (4.1) with a magnetic field given by equation (4.3) and a heating term given by equation (4.5) was studied by Meszaros (1975) and further considered by Ipser and Price (1977, 1982, 1983), Maraschi *et al.* (1979), and Maraschi, Roasio, and Treves (1982).

For low accretion rate, $\dot{\mathfrak{M}} \leq 10^{-7}\ \dot{\mathfrak{M}}_c$, even in the presence of turbulent heating, the radiative processes are inefficient and the results are qualitatively similar to those of Shapiro (1973*a*): the gas heats up quasi-adiabatically and the efficiency is low. At intermediate accretion rates the efficiency increases and opacity effects come into play. The optical depth for synchrotron self-absorption in

the field given by equation (4.3) is for $\nu \lesssim \nu_s$ (Ipser and Price 1982)

$$\tau_{syn} \sim 2 \times 10^5 \left(\frac{\dot{\mathfrak{M}}}{\mathfrak{M}_\odot}\right)^{1/2} \left(\frac{\dot{\mathfrak{M}}}{\dot{\mathfrak{M}}_c}\right)^{1/2} T_{10}^{-5} \left(\frac{r}{r_G}\right)^{3/4} \left(\frac{\nu}{\nu_s}\right)^{-5/3}, \quad (4.6)$$

where T_{10} is the temperature in units of 10^{10} K.

For $\dot{\mathfrak{M}} > 10^{-4} \dot{\mathfrak{M}}_c$, $\tau_{syn} > 1$ and the effects of self-absorption are essential. The efficiency reaches $\sim 10^{-2}$ and the emission peak occurs at the transparency frequency, which can be $10^2 - 10^3\, \nu_s$.

B. *Comptonization*

Another essential effect at large accretion rates is related to the Thomson optical depth, which for free-fall is

$$\tau_T = \int_{r_G}^{\infty} \sigma_T n_e dr = \frac{\dot{\mathfrak{M}}}{\dot{\mathfrak{M}}_c} \left(\frac{r}{r_G}\right)^{-1/2}. \quad (4.7)$$

The outgoing shychrotron photons which initially have $h\nu \ll m_e c^2$ gain energy from the hot electrons through repeated Compton scatterings if τ_T approaches 1. This process is usually called Comptonization (Rybicki and Lightman 1979; Pozdnyakov, Sobol', and Sunyaev 1983). The average energy gain per scattering is

$$\begin{aligned} \Delta h\nu/h\nu &= 4kT/mc^2 \quad \text{(a)} \\ \Delta h\nu/h\nu &= 16\,(kT/mc^2)^2 \quad \text{(b)}, \end{aligned} \quad (4.8)$$

in the nonrelativistic (a) and relativistic (b) limits, respectively. It has been shown both analytically and numerically (Shapiro, Lightman, and Eardley 1976; Pozdnyakov *et al.* 1983) that although the probability of repeated scattering decreases exponentially, it gives rise to an exponentially increasing energy gain. The combination of the two effects yields a power-law energy distribution $F_\nu \propto \nu^{-\alpha}$ up to $h\nu \simeq 3kT$ for initially monochromatic photons which propagate through even modest optical depths of hot gas. Here we report two expressions for the index of the power law derived (a) analytically in the nonrelativistic limit (Sunyaev and Titarchuk 1980), and (b) numerically with relativistic corrections (Pozdnyakov *et al.* 1983; Zdziarski 1985).

$$\alpha = \left(\frac{9}{4} + \frac{\pi^2}{3(\tau_T + \frac{2}{3})^2 \frac{kT}{m_e c^2}}\right)^{1/2} - \frac{3}{2} \quad (4.9a)$$

$$\alpha = -\ln P / \ln\left[1 + 4\frac{kT}{mc^2} + 16\left(\frac{kT}{mc^2}\right)^2\right] \quad (4.9b)$$

$$P = \frac{3}{4}\tau_T \qquad (\tau_T < 1)$$

$$P = 1 - \frac{3}{4\tau_T} \qquad (\tau_T > 1)$$

Comptonization is crucial in all problems in which the accretion rate is nearly critical. Specific model computations including the effects mentioned above were carried out by several authors (e.g., Takahara *et al.* 1981; Maraschi, Roasio, and Treves 1982; Ipser and Price 1982). Maximum temperatures of 10^9–10^{10} K are found and the results agree in finding high efficiencies ($\eta \sim 10^{-1}$) and power-law spectra extending from the synchrotron self-absorption frequency to 3 kT. The derived spectral slope depends on the optical depth, but not too strongly. For a range of two decades $\dot{\mathfrak{M}} = (10^{-2} - 1)\dot{\mathfrak{M}}_c$ in accretion rate, α varies between 1 and 0.5, due to the decrease of the temperature at high optical depths. Examples of temperature profiles and spectra are given in Figures 4 and 5.

C. *Spherical Accretion with Radiation Pressure*

The radiation force on a free electron is $f_{rad} = (\sigma_T/c)\, F$ where F is the radiation flux. Since the electric field strongly couples protons and electrons in the accreting plasma, the resultant force on a volume element of completely ionized hydrogen is

$$\left(\frac{G\mathfrak{M}\mathfrak{m}_p}{r^2} - \frac{\sigma_T}{c}\frac{L(r)}{4\pi r^2}\right)\frac{\rho}{\mathfrak{m}_p}. \quad (4.10)$$

At large distance from the star the outgoing luminosity is constant and the vanishing of the resultant force, which is independent of r, defines the Eddington luminosity

$$L_E = \frac{4\pi G \mathfrak{m}_p c}{\sigma_T}. \quad (4.11)$$

Luminosities of this order are actually observed in accreting sources and it is interesting to discuss how the dynamics are modified. In the case of neutron stars or white dwarfs the accretion rate fixes the outgoing luminosity. In the simplest model (Thomson opacity only) it is found that

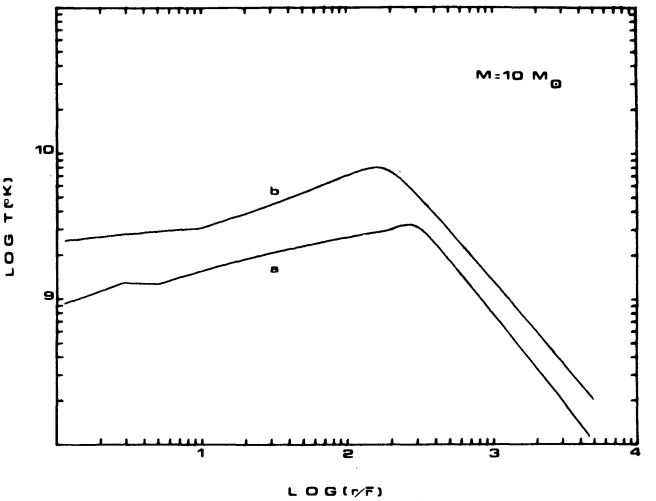

FIG. 4–Temperature profiles around a black hole of 10 $\mathfrak{M}_\odot$ accreting at a rate of 3×10^{18} g s^{-1} (a), and $\dot{\mathfrak{M}} = 3 \times 10^{17}$ g s^{-1} (b) $\langle r \rangle = 3r_G$ (from Maraschi *et al.* 1982).

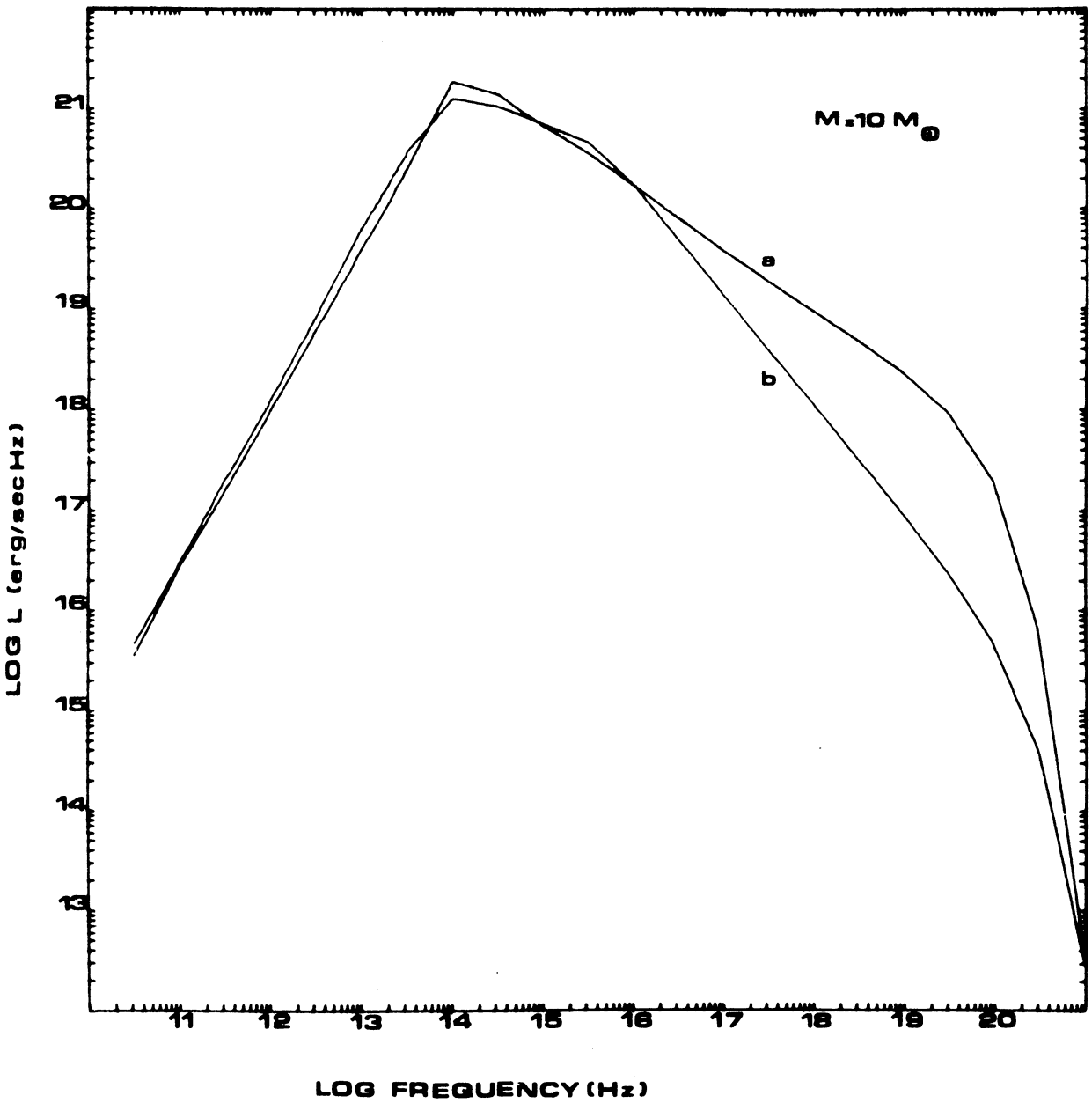

FIG. 5–Spectra from an accreting black hole of 10 $\mathfrak{M}_\odot$, for an accretion rate $\dot{\mathfrak{M}} = 3 \times 10^{18}$ g s^{-1} (a) and $\dot{\mathfrak{M}} = 3 \times 10^{17}$ g s^{-1} (b) $\langle r \rangle = 3r_G$ (from Maraschi *et al.* 1982).

the simplest model (Thomson opacity only) it is found that for $L = \lambda L_E$ with $\lambda \leq 1$ the flow occurs at velocities everywhere lower than free-fall. The infall velocity has a maximum at $r > r_{st}$, and decreases significantly toward the surface of the star (see Fig. 6).

For $\lambda > 1$ no stationary solution exists. Time-dependent solutions have been explored by Cowie, Ostriker, and Stark (1978) and Klein, Stockman, and Chevalier (1980). In the latter investigation, which includes supercritical accretion, an extended envelope is shown to form around the neutron star in 10 to 100 ms.

The case of supercritical accretion onto a black hole is different because of the different inner boundary conditions. The inflow velocity at the horizon as measured by static observers must equal the speed of light. The full hydrodynamic treatment is rather complicated (Thorne, Flammang, and Zytkow (1981); Flammang (1982, 1984)), but confirms the validity of a simple physical concept, the trapping radius (eq. (4.13)), introduced by Rees (1978) and studied in a simple hydrodynamic model by Begelman (1978, 1979). At high accretion rates the radiation transfer, in a first approximation, can be treated diffusively. The photon diffusion velocity at r is $\sim c/\tau(r)$. At the same time photons are convected inward with veloc-

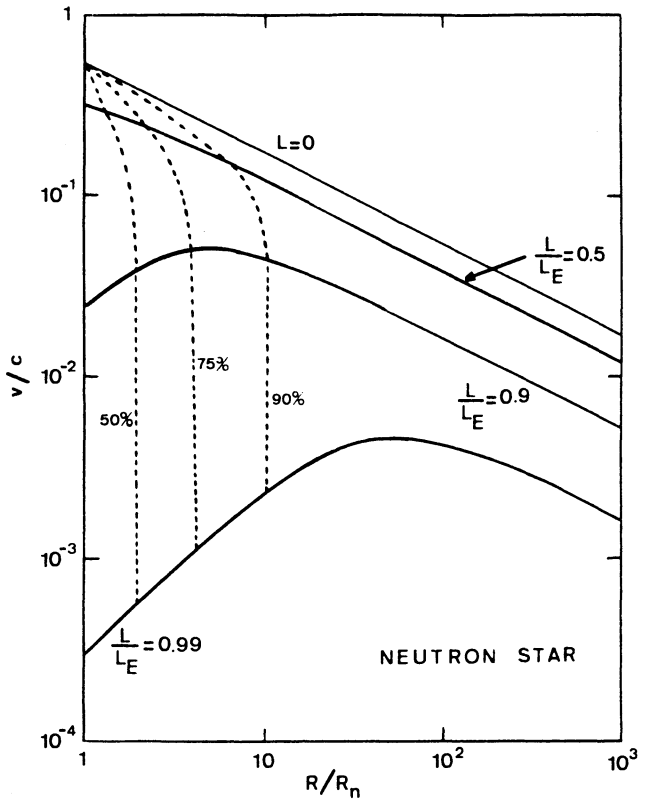

FIG. 6–Velocity profiles for the accretion flow on a neutron star of 1 $\mathfrak{M}_\odot$ and radius $r_{st} = 10^6$ cm, for different outgoing luminosities (from Maraschi *et al.* 1978). The abscissae are measured in star radii.

ity $v(r)$. For

$$v(r) > c/\tau(r) \ , \tag{4.12}$$

convection overwhelms diffusion, so that the radiation emitted by the gas is trapped within it and falls toward the black hole. Assuming that $v(r)$ is given by free-fall, i.e., $v(r) = c(r/r_G)^{-1/2}$, and taking expression (4.7) for the optical depth, one finds that equation (4.12) is valid when $r > r_{tr}$, where

$$r_{tr} = \frac{\dot{\mathfrak{M}}}{\dot{\mathfrak{M}}_c} r_G \ . \tag{4.13}$$

It can be shown that the luminosity reaching the observer at infinity, L_∞, apart from minor corrections, is simply the luminosity produced at $r \geq r_{tr}$. If this is some fraction λ of the gravitational power at r_{tr},

$$L_\infty = L(> r_{tr}) = \lambda \frac{G\mathfrak{M}\dot{\mathfrak{M}}}{r_{tr}} \ , \tag{4.14}$$

and using the definition of equation (4.13) one finds

$$L_\infty = \lambda \frac{4\pi G \mathfrak{M} m_p c}{\sigma_T} = \lambda L_E \ . \tag{4.15}$$

Hence, whatever the accretion rate, the emerging luminosity is limited to a fraction of the Eddington luminosity. This is shown with a rigorous semianalytic treatment of Comptonization in a spherical flow by Colpi (1988). The effect is increased if $e^+ - e^-$ pair production contributes to the opacity (Lightman, Zdziarski, and Rees 1987).

The determination of the accretion rate, given the external boundary conditions is a different problem and requires a discussion of the critical points in the flow (see, e.g., Turolla, Nobili, and Calvani 1986).

D. *Two-Temperature Accretion*

In the previous section it was assumed that the accreting plasma was in thermal equilibrium, i.e., that the distribution functions of electrons and protons are described by Maxwellians with the same temperature. The relaxation times through Coulomb collisions and their scaling with distance in the spherical case are discussed, e.g., by Colpi, Maraschi, and Treves (1984). Under reasonable astrophysical conditions, the time required to achieve thermal equilibrium between the ions and electrons can be longer than the dynamical time scale (i.e., the free-fall time scale). Therefore, electrons and ions can be assumed to behave as independent fluids. This approach has been used both in spherical and disk models (e.g., Colpi *et al.* 1984; Colpi, Maraschi, and Treves 1986; Shapiro, Lightman, and Eardley 1976; Rees *et al.* 1982). Because protons are inefficient radiators they reach temperatures of the order of the virial temperature (eq. (2.17)) and dominate the pressure of the fluid, while the electrons, due to strong radiative losses, attain much lower temperatures. Therefore, the dynamical properties of the flow are determined by the protons and the radiative properties by the electrons. This situation may occur at accretion rates below the critical one and gives rise to interesting models, where the high ion temperature can be used to confine jets or to produce high-energy radiation (gamma rays).

It should be noted, however, that the coupling between electrons and ions could be much more efficient than the Coulomb one, as one can argue on the basis of collective plasma effects, which should be present in turbulent magnetic fields (Begelman and Chiueh 1987). In this case the temperatures of the two populations would be close, and the single temperature description would be realistic.

V. Accretion Disks

In many astrophysical situations the accreted matter has substantial angular momentum. This completely changes the physical picture of accretion discussed in the previous sections. The most important process governing the accretion of rotating matter is the action of viscous stresses. Gas orbiting a compact central object gradually loses its angular momentum through viscous stresses (friction) to gas further out. With friction, energy is also dissipated and the inner gas spirals further inward. Viscous stresses not only drive accretion by transporting mass inward and angular momentum outward but also

convert the gravitational energy of matter into heat. The heat diffuses toward the top and bottom surfaces of the flow where it is radiated away. Radiation from the hot innermost parts can be absorbed by much cooler outer regions and heat them up, forming a tenuous corona and blowing off a wind. If the central accreting object has a rigid surface a shock is formed close to it (see Section III for the spherical case). Black-hole accretion, on the other hand, is highly supersonic in the innermost part. Presence of a strong magnetic field is another complication.

There is no complete, satisfactory theoretical model of this rather-complex hydrodynamical situation. Advanced numerical codes are still not powerful enough to cope with it, and our present understanding of accretion of rotating matter is based on a very approximate, semianalytic approach. In particular, we refer to the papers of Prendergast and Burbidge (1968), Shakura (1972), Pringle and Rees (1972), Shakura and Sunyaev (1973), and Pringle (1981). We shall now present the basic assumptions using cylindrical coordinates: R (horizontal), Z (vertical), and φ (azimuthal). The geometrical half-thickness of the flow $H = H(R)$, the angular velocity Ω, and the surface density of matter

$$\Sigma(R) = 2\int_0^H \rho(R,Z)dZ \ , \tag{5.1}$$

appear in some of these assumptions.

GEOMETRY. The flow is axially symmetric and plane symmetric: its properties do not depend on φ and depend on Z only through $|Z|$. The vertical thickness is very small, $H \ll R$.

KINEMATICS. Azimuthal rotation agrees with the circular Keplerian motion

$$V_\varphi = \Omega R = V_k = (G\mathfrak{M}/R)^{1/2} \ . \tag{5.2}$$

Only this motion contributes to shear $\sigma = 1/2\, R(d\Omega/dR)$. This expression for the shear is valid when the angular velocity is independent of Z. (For a general definition see, e.g., Landau and Lifshitz 1959.) The horizontal component of velocity is very subsonic

$$V_R < V_s = \left(\frac{\partial p}{\partial \rho}\right)^{1/2} \ .$$

The vertical component is negligible

$$V_Z \ll V_R \ll V_\varphi \ .$$

DYNAMICS. The horizontal pressure gradient is negligible. At the inner edge of the accretion flow $R = R_{in}$ the viscous torque vanishes and the accretion rate is much smaller than the critical one $\dot{\mathfrak{M}} \ll \dot{\mathfrak{M}}_c$.

DISSIPATION. The horizontal heat flux is negligible. The Z-averaged kinematic viscosity,

$$\langle \nu \rangle = \frac{1}{\Sigma(R)}\int_0^H \rho(R,Z)\nu(R,Z) \ , \tag{5.3}$$

is given by the formula

$$\langle \nu \rangle = \alpha V_s H \ , \tag{5.4}$$

where $\alpha = \text{const}$ is a phenomenological viscosity coefficient. The opacity is dominated by electron scattering:

$$\kappa = \kappa_{es} = 0.4 \text{ g cm}^{-2} \ . \tag{5.5}$$

These assumptions define the standard α model of thin accretion disks: "α" because the assumption of equation (5.4) is crucial (and restrictive!) and "thin disk" because with $H/R \ll 1$ the flow shape resembles a thin disk. The action of viscous stresses is so important for the theory of accretion disks that our discussion must start from this point.

Consider a particular cylindrical surface $R = R_0$, crossing the accretion flow. The rates of mass and angular-momentum flow across this surface are $\dot{\mathfrak{M}}(R_0)$ and $\dot{J}(R_0)$:

$$\dot{J}(R_0) = \dot{\mathfrak{M}}(R_0)l(R_0) - g(R_0) \ , \tag{5.6}$$

with l being the specific angular momentum and $g(R_0)$ the viscous torque acting through $R = R_0$:

$$g(R_0) = 2\pi \int R_0^3 \left(\frac{d\Omega}{dR}\right)_{R_0} \rho(R_0,Z)\nu(R_0,Z)dZ$$

$$= 2\pi R_0^3 \left(\frac{d\Omega}{dR}\right)_{R_0} \Sigma(R_0)\langle \nu \rangle(R_0) \ . \tag{5.7}$$

When $(d\Omega/dR) > 0$ the viscous torque transports the angular momentum outward. At the inner edge $R = R_{in}$ the torque vanishes, $g(R_{in}) = 0$, and therefore

$$\dot{J}(R_{in}) = \dot{\mathfrak{M}}(R_{in})l(R_{in}) \ . \tag{5.8}$$

In the stationary accretion disk the rate of mass and angular-momentum flow across any $R = R_0$ cylinder must be the same, they do not depend on R.

For a stationary disk,

$$\dot{\mathfrak{M}}(R) = \dot{\mathfrak{M}}_0 = \text{const}, \qquad \dot{J}(R) = J_0 = \text{const} \ . \tag{5.9}$$

From equations (5.6), (5.8), and (5.9) it follows that in the stationary accretion disk

$$\dot{\mathfrak{M}}_0[l(R) - l(R_{in})] = 2\pi R^3 \left(\frac{d\Omega}{dR}\right)\Sigma\langle \nu \rangle \ . \tag{5.10}$$

When rotation is given by the Keplerian law, (eq. (5.2)), then the last formula reads

$$3\pi\langle \nu \rangle \Sigma = \dot{\mathfrak{M}} f \tag{5.11}$$

$$f = \frac{l(R) - l(R_{in})}{l(R)} = 1 - \left(\frac{R_{in}}{R}\right)^{1/2} \ . \tag{5.12}$$

The viscous stresses acting inside a mass M dissipate the kinetic energy and transform it to heat at the rate (Landau

and Lifshitz 1959)

$$\dot{E} = 4\int_0^M \sigma^2 \nu dM = \int\int 2\pi R^3 \left(\frac{d\Omega}{dR}\right) \nu\rho dR dZ \quad . \quad (5.13)$$

For a mass inside an infinitesimal shell between $R = R_0$ and $R = R_0 + dR$ the last formula gives

$$Q^+(R) = \frac{1}{2\pi R}\frac{d\dot{E}}{dR} = \left(R\frac{d\Omega}{dR}\right)^2 \int \nu\rho dZ = \left(R\frac{d\Omega}{dR}\right)^2 \Sigma\nu$$

$$Q^+(R) = \frac{1}{2\pi R}\left[l(R) - l(R_{\rm in})\right]\frac{d\Omega}{dR} \quad . \quad (5.14)$$

The quantity Q^+ is the surface heat-generation rate due to viscous processes. When rotation is Keplerian it is equal to

$$Q^+(R) = \frac{3G\mathfrak{M}\dot{\mathfrak{M}}}{4\pi R^3} f \quad . \quad (5.15)$$

All the equations basic to the accretion disk theory are collected in Table II and will be referred to with brackets. They are written in a simplified form apt to further generalization. Most of them are self-explanatory. For example, equation [2] approximates the hydrostatic equilibrium condition

$$\frac{1}{\rho}\frac{dP}{dZ} = \frac{d}{dz}\left[-\frac{G\mathfrak{M}}{(R^2+Z^2)^{1/2}}\right] \quad . \quad (5.16)$$

In a similar way equation [7] approximates, for the optically thick case,

$$Q^- = -\frac{c}{3}\frac{d(aT^4)}{d\tau} \quad , \quad \tau = \int K\rho dZ \quad . \quad (5.17)$$

Table I gives the list of all the relevant accretion-disk structure quantities. Tables I and II contain all the information relevant to the standard α models of thin accretion disks.

There are 20 equations for 24 physical quantities. Therefore, four physical quantities are independent. It is convenient to use

$$\mathfrak{M}, \dot{\mathfrak{M}}, R, \alpha \quad (5.18)$$

as the four independent quantities.

All the equations for the standard disk model in Table II, with the exception of equation [11], are linear in their logarithmic version. Even equation [11] is linear in the two asymptotic cases in which either the gas pressure

$$P_{\rm gas} = \frac{k}{m_p}\frac{T}{\langle\mu\rangle} \quad ,$$

or the radiation pressure $P_{\rm rad} = 1/3\, aT^4$ dominates. In the first case $\beta \simeq 1$; in the second case $\beta \simeq 0$ with β defined by

$$\beta = \frac{P_{\rm gas}}{P} = \frac{P_{\rm gas}}{P_{\rm gas} + P_{\rm rad}} \quad . \quad (5.19)$$

Therefore, in the two asymptotic cases it is possible to write down an analytic solution for the standard accretion-disk structure. This was done first by Shakura and Sunyaev (1973). We present the Shakura-Sunyaev solution in a slightly modified version, better suited to astrophysical applications.

For the case of $P_{\rm rad} \ll P_{\rm gas}$:

$$\Sigma = 7.08 \times 10^4\, \alpha^{-4/5} f^{3/5} (R/R_G)^{-3/5} \times (\mathfrak{M}/\mathfrak{M}_\odot)^{1/5} (\dot{\mathfrak{M}}/\dot{\mathfrak{M}}_c)^{3/5} \quad [\mathrm{g/cm^2}] \quad (5.20)$$

$$H/R = 1.15 \times 10^{-2}\, \alpha^{-1/10} f^{1/5} (\mathfrak{M}/\mathfrak{M}_\odot)^{1/10} \times (\dot{\mathfrak{M}}/\dot{\mathfrak{M}}_c)^{1/5} \quad (5.21)$$

$$\rho = 1.03 \times 10\alpha^{-7/10} f^{2/5} (R/R_G)^{-33/20} \times (\mathfrak{M}/\mathfrak{M}_\odot)^{-7/10} (\dot{\mathfrak{M}}/\dot{\mathfrak{M}}_c)^{2/5} \quad [\mathrm{g/cm^3}] \quad (5.22)$$

$$P = 3.01 \times 10^{17}\, \alpha^{-9/10} f^{4/5} (R/R_G)^{-51/20} \times (\mathfrak{M}/\mathfrak{M}_\odot)^{-9/10} (\dot{\mathfrak{M}}/\dot{\mathfrak{M}}_c)^{4/5} \quad [\mathrm{dyn/cm^2}] \quad (5.23)$$

$$T = 3.53 \times 10^8\, \alpha^{-1/5} f^{2/5} (R/R_G)^{-9/10} \times (\mathfrak{M}/\mathfrak{M}_\odot)^{-1/5} (\dot{\mathfrak{M}}/\dot{\mathfrak{M}}_c)^{2/5} \quad [\mathrm{K}] \quad (5.24)$$

$$\frac{V}{c} = 3.5 \times 10^{-5}\, \alpha^{4/5} f^{-3/5} (R/R_G)^{-2/5} \times (\mathfrak{M}/\mathfrak{M}_\odot)^{-1/5} (\dot{\mathfrak{M}}/\dot{\mathfrak{M}}_c)^{2/5} \quad (5.25)$$

$$F = 8.3 \times 10^{25} f (R/R_G)^{-3} (\mathfrak{M}/\mathfrak{M}_\odot)^{-1} (\dot{\mathfrak{M}}/\dot{\mathfrak{M}}_c) \quad [\mathrm{erg/cm^2 s}] \quad . \quad (5.26)$$

For the case $P_{\rm gas} \ll P_{\rm rad}$:

$$\Sigma = 4.24\, \alpha^{-1} f^{-1} (R/R_G)^{3/2} (\dot{\mathfrak{M}}/\dot{\mathfrak{M}}_c)^{-1} \quad [\mathrm{g/cm^2}] \quad (5.27)$$

$$\frac{H}{R} = 0.74 f (R/R_G)^{-1} (\dot{\mathfrak{M}}/\dot{\mathfrak{M}}_c) \quad (5.28)$$

$$\rho = 9.51 \times 10^{-6}\, \alpha^{-1} f^{-2} (R/R_G)^{3/2} \times (\mathfrak{M}/\mathfrak{M}_\odot)^{-1} (\dot{\mathfrak{M}}/\dot{\mathfrak{M}}_c)^{-2} \quad [\mathrm{g/cm^3}] \quad (5.29)$$

$$P = 2.33 \times 10^{15}\, \alpha^{-1} (R/R_G)^{-3/2} \times (\mathfrak{M}/\mathfrak{M}_\odot)^{-1} \quad [\mathrm{dyn/cm^2}] \quad (5.30)$$

$$T = 3.10 \times 10^7\, \alpha^{-1/4} (R/R_G)^{-3/8} \times (\mathfrak{M}/\mathfrak{M}_\odot)^{-1/4} \quad [\mathrm{K}] \quad (5.31)$$

$$\frac{V}{c} = 0.53\, \alpha f (R/R_G)^{-5/2} (\dot{\mathfrak{M}}/\dot{\mathfrak{M}}_c) \quad (5.32)$$

$$F = 8.3 \times 10^{25} f (R/R_G)^{-3} (\mathfrak{M}/\mathfrak{M}_\odot)^{-1} \times (\dot{\mathfrak{M}}/\dot{\mathfrak{M}}_c) \quad [\mathrm{erg/cm^2 s}] \quad . \quad (5.33)$$

The boundary between the two regions is within the radii derived in the two regimes

$$\frac{R}{R_G} = 6.4 \times 10^3\, \alpha^{2/11} f^{-16/11} (\mathfrak{M}/\mathfrak{M}_\odot)^{2/11} \times (\dot{\mathfrak{M}}/\dot{\mathfrak{M}}_c)^{16/11} \quad (5.34)$$

$$\frac{R}{R_G} = 78.6\, \alpha^{2/21} f^{-16/21} (\mathfrak{M}/\mathfrak{M}_\odot)^{2/21} (\dot{\mathfrak{M}}/\dot{\mathfrak{M}}_c)^{16/21} \quad . \quad (5.35)$$

The inner region is that dominated by radiation pressure and its extension increases with the accretion rate. To complete the solution one should compute the case $P_{\rm gas} \sim P_{\rm rad}$ numerically.

TABLE II

List of the Accretion Disk Structure Equations

[1]	$\Sigma = 2H\rho$	definition of surface density
[2]	$\frac{H}{R} = \frac{V_s}{V_k}$	vertical hydrostatic equilibrium
[3]	$V_s^2 = \frac{P}{\rho}$	sound velocity
[4]	$\dot{M} = 2\pi R\Sigma V$	mass conservation
[5]	$Q^+ = \frac{1}{2\pi R} l \frac{d\Omega}{dR} f\dot{M} \overset{*}{=} \frac{3GM\dot{M}f}{4\pi R^3}$	viscous heat production rate
[6]	$\pi\nu\Sigma = \frac{1}{2}\dot{M}fl\left(\frac{d\Omega}{dR}\right)^{-1} \overset{*}{=} \frac{1}{3}\dot{M}f$	angular momentum balance
[7]	$Q^- = \frac{4\alpha c T^4}{3\rho H k}$	heat loss (optically thick case)
[8]	$F = \frac{1}{2}Q^-$	radiation flux
[9]	$Q^+ = Q^- + q$	heat balance
[10]	$\nu = \alpha V_s H$	viscosity law
[11]	$P = \frac{\rho}{\mu m_p}\rho T + \frac{1}{3}aT^4$	equation of state
[12]	$f = \frac{\epsilon - l(R_{in})}{l} \overset{*}{=} 1 - \left(\frac{R_{in}}{R}\right)^{1/2}$	radial function
[13]	$\Omega = \frac{l}{R^2}$	angular velocity
[14]	$V_\varphi = \frac{l}{R}$	azimuthal velocity
[15]	$R_{in} = R_{in}(\ldots) \overset{*}{=} \frac{6GM}{c^2}$	inner edge
[16]	$V_\varphi = V_\varphi(\ldots) \overset{*}{=} V_k$	azimuthal velocity
[17]	$q = q(\ldots) \overset{*}{=} O$	horizontal heat flux
[18]	$\alpha = \alpha(\ldots) \overset{*}{=} \text{const}$	viscosity law
[19]	$\kappa = \kappa(\ldots) \overset{*}{=} \kappa_{es}$	opacity
[20]	$V_k = \left(\frac{GM}{R}\right)^{1/2}$	Keplerian velocity

The symbol $\overset{*}{=}$ indicates equality valid only in the case of the standard disk model. Other equalities are more general. The location of the inner edge in the table refers to the black hole accretion (onto a nonrotating hole).

A. *Single Disk with Fixed Accretion Rate*

We shall discuss, as an example, two disk models with $\mathfrak{M} = 10\,\mathfrak{M}_\odot$ and $\mathfrak{M} = 10^8\,\mathfrak{M}_\odot$ central black holes, both having $\alpha = 0.1$ and $\dot{\mathfrak{M}}/\dot{\mathfrak{M}}_c = 0.1$. The functions $T(R)$ and

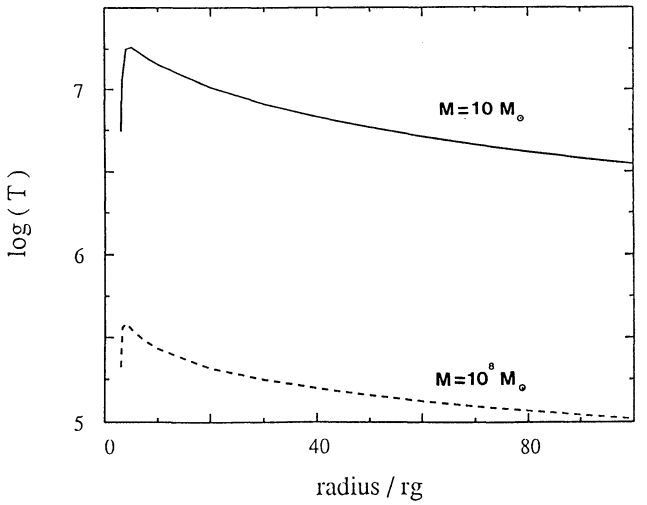

FIG. 7(a)–Equatorial temperature (K) profile for $\dot{\mathfrak{M}} = 0.1\,\dot{\mathfrak{M}}_c$, $\alpha = 0.1$, $\mathfrak{M} = 10\,\mathfrak{M}_\odot$ (upper curve) $\dot{\mathfrak{M}} = 0.1\,\dot{\mathfrak{M}}_c$, $\alpha = 0.1$, $\mathfrak{M} = 10^8\,\mathfrak{M}_\odot$ (lower curve).

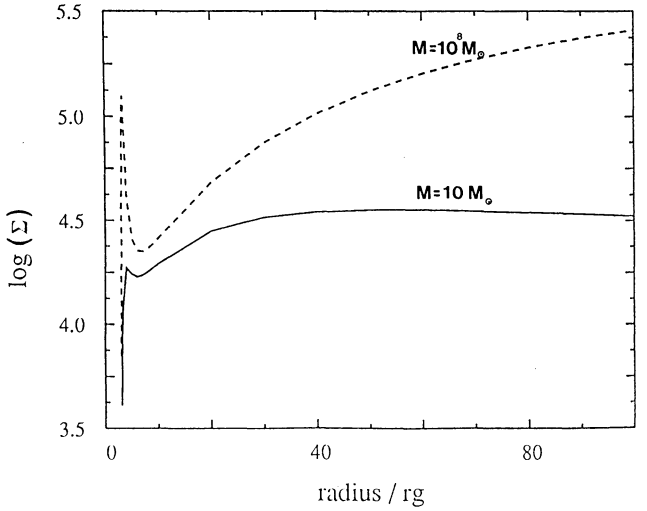

FIG. 7(b)–Surface density (g cm^{-2}) profile for $\dot{\mathfrak{M}} = 0.1\,\dot{\mathfrak{M}}_c$, $\alpha = 0.1$, $\mathfrak{M} = 10\,\mathfrak{M}_\odot$ (lower curve) $\mathfrak{M} = 0.1\,\dot{\mathfrak{M}}_c$, $\alpha = 0.1$, $\mathfrak{M} = 10^8\,\mathfrak{M}_\odot$ (upper curve).

$\Sigma(R)$ are shown in Figures 7(a) and 7(b). The temperature peaks at about $R = 2\,R_{in}$ because there $dQ^+/dR = 0$ independently of $\dot{\mathfrak{M}}$, $\mathfrak{M}$, and α.

The temperature at the peak is

$$T_{max} \sim 10^7 \left(\frac{\mathfrak{M}}{\mathfrak{M}_\odot}\right)^{-1/4} \left(\frac{\dot{\mathfrak{M}}}{\dot{\mathfrak{M}}_c}\right)^{1/4} \quad [\mathrm{K}] \ . \qquad (5.36)$$

The thermal radiation connected with this temperature has maximal frequency $\nu_{max} = kT_{max}/h$ which equals

$$h\nu_{max} \simeq \left(\frac{\mathfrak{M}}{\mathfrak{M}_\odot}\right)^{1/4} \left(\frac{\dot{\mathfrak{M}}}{\dot{\mathfrak{M}}_c}\right)^{1/4} \quad [\mathrm{keV}] \ . \qquad (5.37)$$

Therefore, optical and X-ray thermal photons can be produced by accretion disks around not-very-massive black holes ($\mathfrak{M} \simeq 10\,\mathfrak{M}_\odot$). Accretion onto supermassive black holes ($\mathfrak{M} \sim 10^8\,\mathfrak{M}_\odot$) can produce optical and ultraviolet photons. These and the following estimates refer to the optically thick case.

The temperature at the outer parts of the disk ($R/R_{in} \to \infty$) is given by

$$T_{out}(R) \simeq 5 \times 10^7 \left(\frac{\mathfrak{M}}{\mathfrak{M}_\odot}\right)^{-1/4} \left(\frac{\dot{\mathfrak{M}}}{\dot{\mathfrak{M}}_c}\right) \left(\frac{R}{R_{in}}\right)^{3/4} \ . \qquad (5.38)$$

At a given radius one can assume the Planck formula (blackbody radiation) for the thermal spectrum, $S_\nu(\nu,T)$, with the temperature corresponding to this radius: for small frequencies (Rayleigh Jeans) $S_\nu \sim \nu^2$, and for the high ones $S_\nu \sim \nu^3 e^{-h\nu/kT}$. Integrating this over the whole disk one gets the approximate shape of the standard spectrum. The contributions from different disk regions form two parts, one called blackbody disk spectrum, which behaves like $\nu^{1/3}$, and the other one called modified blackbody with the behavior like ν^0 (e.g., Novikov and Thorne 1973). In real situations the spectrum can be strongly influenced by the detailed radiative processes, which occur at the optically thin part of the disk (e.g., corona).

B. *Sequences of the Disk Models, with Varying Accretion Rate*

Figure 8(a) shows the relation between $\dot{\mathfrak{M}}$ and Σ for a sequence of models with $R = 5\,R_G$, $\alpha = 1$, and $\mathfrak{M} = 10^5$, 10^6, 10^7, $10^8\,\mathfrak{M}_\odot$. For the high accretion rates all the curves converge to a unique line, which asymptotically agrees with the approximate solution (eq. (4.27)). This is because there is no mass dependence there. The turning point of the $\dot{\mathfrak{M}}(\Sigma)$ curves always corresponds to $\beta = 2/5$, because

$$\frac{d\ln\Sigma}{d\ln\dot{\mathfrak{M}}} = 5\,\frac{\beta - 2/5}{2 + 3\beta} \ . \qquad (5.39)$$

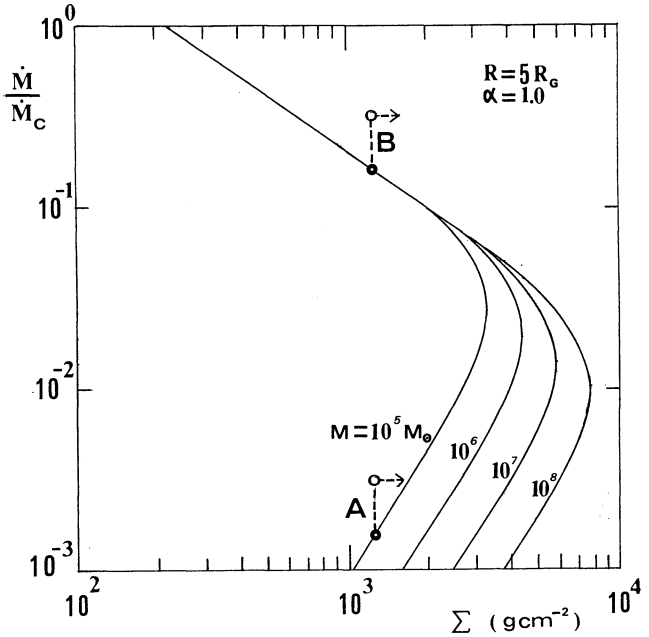

FIG. 8(a)–The sequence of standard disk accretion models for different masses of the black hole. $R = 5\,R_G$, $\alpha = 1.0$.

Its location in terms of $\dot{\mathfrak{M}}/\dot{\mathfrak{M}}_c$ depends very weakly on $\mathfrak{M}$ and α: the turning point

$$\left(\frac{\dot{\mathfrak{M}}}{\dot{\mathfrak{M}}_c}\right) = 3.4\times10^{-3} f^{-1}\left(\frac{R}{R_G}\right)^{21/16}\alpha^{-1/8}\left(\frac{\mathfrak{M}}{\mathfrak{M}_\odot}\right)^{-1/8} . \quad (5.40)$$

C. *Stability*

We shall now show how the stability of standard models relates to the slope of the $\dot{\mathfrak{M}}(\Sigma)$ curve. Let us start with an argument which, although not quite formal, gives a quick insight into the nature of the problem (compare Bath and Pringle 1981). In Figure 8(a) the points A and B (open dots) lie above the equilibrium sequence. They can represent a perturbation of equilibrium models indicated by black dots. Thus, in both cases, the perturbed models have too high accretion rates, $\dot{\mathfrak{M}}$ (perturbed) > $\dot{\mathfrak{M}}$ (equilibrium). They are oversupplied with matter, and therefore their surface densities must increase, which shifts them to the right as indicated by arrows. This brings the model A, connected with a positive slope of the $\dot{\mathfrak{M}}(\Sigma)$ curve, back to equilibrium, indicating that the model A is stable. Model B goes further off the equilibrium curve and it is unstable. From the results of Piran (1978) one can obtain that

$$\frac{d\ln\dot{\mathfrak{M}}}{d\ln\Sigma} > 0 \quad (5.41)$$

is both sufficient and necessary for viscous stability. Piran introduced the phenomenological parameters $\mathcal{H}$, $\mathcal{L}$, $\mathcal{M}$, $\mathcal{N}$ to describe dissipative processes:

$$\mathcal{H} \equiv \left(\frac{\partial\ln Q^-}{\partial\ln H}\right)_\Sigma \qquad \mathcal{L} = \left(\frac{\partial\ln Q^-}{\partial\ln\Sigma}\right)_H$$

$$\mathcal{M} \equiv \left(\frac{\partial\ln Q^+}{\partial\ln H}\right)_\Sigma \qquad \mathcal{N} = \left(\frac{\partial\ln Q^+}{\partial\ln\Sigma}\right)_H . \quad (5.42)$$

In the case of the standard disk model these coefficients have well-determined values,

$$\mathcal{H}=4\frac{1+\beta}{4-3\beta};\quad \mathcal{L}=\frac{-\beta}{4-3\beta},\quad \mathcal{M}=2,\quad \mathcal{N}=1 , \quad (5.43)$$

but it would be convenient to give general criteria here, in which these coefficients are arbitrary.

The general stability criteria found by Piran can be written in such a way that they directly correspond to the thermal stability criterion

$$\mathcal{H} - \mathcal{M} > 0 , \quad (5.44)$$

and the viscous stability criterion

$$\frac{\mathcal{N}\mathcal{H} - \mathcal{M}\mathcal{L}}{\mathcal{H} - \mathcal{M}} > 0 . \quad (5.45)$$

For stable disk models any of these conditions is necessary, but only two of them together are sufficient for stability. Because in the case of the standard thin-disk model $\mathcal{N}\mathcal{H} - \mathcal{M}\mathcal{L} = (4 + 6\beta)/(4 - 3\beta)$ is positive, the necessary and sufficient criterion for both thermal and viscous instabilities is either of the three equivalent conditions:

$$\left[\mathcal{H} - \mathcal{M} > 0\right] \Leftrightarrow \left[\beta > 2/5\right] \Leftrightarrow \left[d\ln\dot{\mathfrak{M}}/d\ln\Sigma > 0\right] . \quad (5.46)$$

This formally proves our point.

Thermal Instabilities. When equation (5.46) is not fulfilled, thermal perturbations grow exponentially. In the limit of wavelength of the perturbation Λ going to infinity, $\Lambda/H \gg 1$, the rising time does not depend on the wavelength. It is equal to

$$T_{th} = t_{th}\frac{56 - 57\beta - 3\beta^2}{30(2/5 - \beta)} . \quad (5.47)$$

Here t_{th} is the characteristic time for thermal processes

$$t_{th} = 2\pi/\Omega\alpha . \quad (5.48)$$

This type of instability was discovered and studied by Pringle, Rees, and Pacholczyk (1973) and Shakura and Sunyaev (1976).

Viscous Instability. When equation (5.44) is not also fulfilled viscous instabilities grow exponentially at the rate (for $\Lambda/H \gg 1$)

$$T_{vis} = t_{vis}\left(\frac{\Lambda}{R}\right)^2\frac{3}{10}\frac{2 - 3\beta}{2/5 - \beta} . \quad (5.49)$$

Here t_{vis} is the characteristic time for viscous processes:

$$t_{vis} = \frac{t_{th}}{(H/R)^2} . \quad (5.50)$$

This type of instability was found by Lightman and Eardley (1974) and Lightman (1974).

D. *Possibility of a Limit-Cycle Behavior*

The equations describing the standard α disk models (with α = const, $k = k_{es}$ = const, $q = 0$) are all linear in their logarithmic versions with the sole exception of the equation of state [11].

We have seen that the nonlinearity causes the $\dot{\mathfrak{M}}(\Sigma)$ curves describing equilibrium sequences of models (at a given radius) to bend. At the turning points the stability properties change, as a positive slope of $\dot{\mathfrak{M}}(\Sigma)$ corresponds to stable and a negative slope to unstable disk models. Abramowicz *et al.* (1987) have recently shown that the $\dot{\mathfrak{M}}(\Sigma)$ curve bends again, to form another stable branch, at higher accretion rates $\dot{\mathfrak{M}} \sim \dot{\mathfrak{M}}_c$. This bending is also due to additional nonlinearity, connected with a new cooling mechanism operating at $\dot{\mathfrak{M}} \sim \dot{\mathfrak{M}}_c$. In this case the Shakura-Sunyaev model is not adequate and one must consider its modifications to include horizontal pressure gradients and horizontal heat transport (Maraschi, Reina, and Treves 1974). Thus the $\dot{\mathfrak{M}}(\Sigma)$ curve is characteristi-

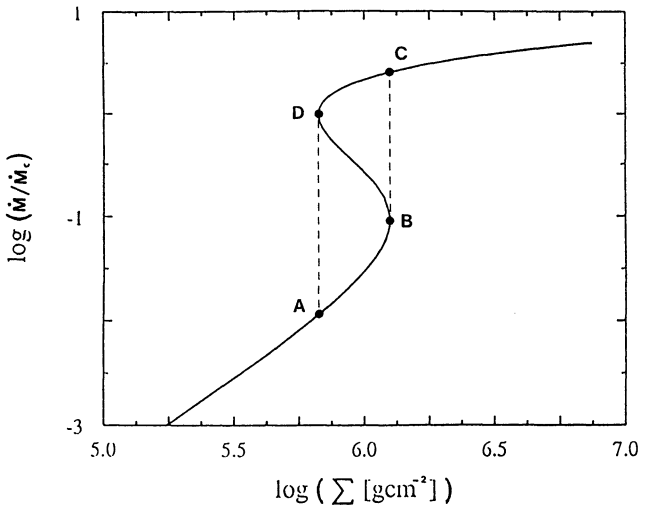

FIG. 8(b)–Limit cycle behavior $\mathfrak{M} = 10\,\mathfrak{M}_\odot$, $\alpha = 1$, $R = 5\,R_G$.

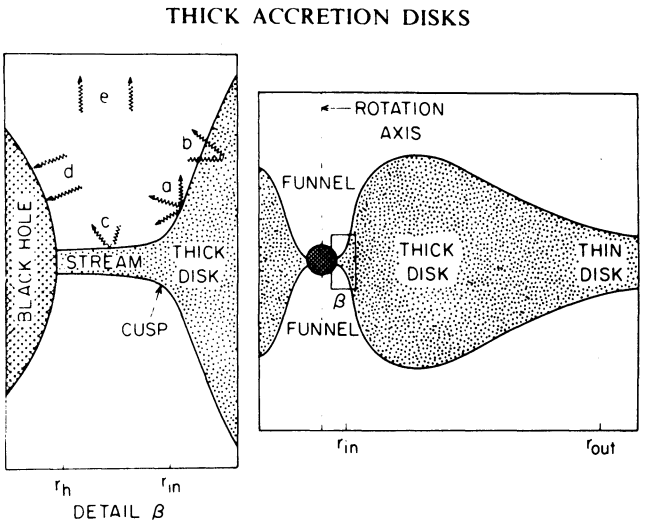

FIG. 9–A sketch of a thick accretion disk (from Abramowicz *et al.* 1980).

cally S-shaped with the upper and lower branches corresponding to stable and the middle branch to unstable disk models. Bath and Pringle (1983) were the first to notice the similarity of this situation to the one known in nonlinear dynamics, where an S-shaped phase portrait of a system indicates a limit-cycle behavior.

If the accretion rate fixed by some outside condition lies in the instability strip (region AB of Fig. 8(b)), then stationary accretion is impossible. Consider point A. The accretion rate is smaller than the supply rate causing local oversupply and an increase of surface density. The disk must evolve in the direction indicated by the arrow up to point B from which further evolution is only possible after a jump to C. Here, however, the accretion rate is higher than the supply rate. The surface density now decreases and the disk evolves down to point D, where another jump, to A, must take place. This closes the cycle.

Such limit-cycle behavior is observed in accretion disks in dwarf novae (see Section VII).

VI. Basics of Thick Accretion Disks

As shown in the previous section (in particular eqs. (5.21) and (5.28)), the geometrical thickness of the disk $H(R)$ becomes comparable to the radius R at the inner boundary of the disk, if the accretion rate is such as to produce a luminosity of the order of the Eddington one. A crucial assumption of the standard disk model, i.e., the disk thinness, becomes invalid; hence, the necessity of models for geometrically thick disks. These have been proposed originally by Paczinski and Wiita (1980) and Jaroszynski, Abramowicz, and Paczynski (1980).

As explained by Abramowicz, Calvani, and Nobili (1980), super-Eddington luminosities do not imply any dramatic consequences for the equilibrium structure of disks, in particular no strong winds as a general property. On the other hand, the high luminosity implies that the horizontal pressure gradient, neglected in the standard model, becomes dynamically important, so that the Keplerian approximation breaks down (e.g., Maraschi *et al.* 1974).

For a wide class of non-Keplerian angular momentum distributions the inner part of the disk can form a toroidal structure, in some cases resembling a sphere with two deep and narrow funnels along the rotation axis (see Fig. 9).

The physics of thick disks is more complex than that of thin disks: assuming that axially symmetric thin disks are one dimensional, we find that the horizontal and vertical structures separate, and disk models are described by ordinary differential equations, exactly integrable in the general stationary case. The stationary equilibria are therefore always given by a set of algebraic equations. As we have discussed already in the previous section, they are linear in the asymptotic cases when either the gas pressure or the radiation pressure dominates, the opacity is given by Thomson scattering or free-free absorption, and the viscosity law is the Shakura-Sunyaev form (eq. (5.4)). In these cases one has an explicit analytic solution in the deep interior of the disk, i.e., in the equatorial plane. Every physical quantity is expressed in terms of three control parameters: viscosity, accretion rate, and mass of the central object $\mathfrak{M}$ (and the distance from the center R). The dependence on the vertical coordinate Z follows from the physical boundary conditions on the surface $Z = H(R)$ and the fact that $H \ll R$ everywhere.

The deep interior of a thick disk is, on the contrary, an extended region. Its structure is described by rather complicated partial-differential equations. The complexity is caused by (a) a priori unknown angular momentum—the angular momentum cannot be assumed Keplerian as for the thin disk, (b) importance of the horizontal gradients of pressure and temperature, and (c) nonlocal

heat balances. Note that all these effects are also important very close to the inner edge of thin disks around compact objects, but they are ignored in the standard model. In the following we will quote some of the main results of the theory of thick disks, referring to Abramowicz *et al.* (1980) for a detailed treatment.

The most complex part of a super-Eddington accretion flow is located near the central compact object. In particular, for accretion onto a black hole (or a neutron star), a self-crossing equipotential surface—the Roche lobe—which has the shape of a cusp, exists due to general relativistic gravity competing with the disk rotation (see Abramowicz *et al.* 1980). The location of the cusp $R = R_{in}$ follows from the condition that the Keplerian angular momentum at $R = R_{in}$ (given by the gravity of the hole) equals the angular momentum of the rotating matter there. The nonzero thickness of the disk in the cusp implies Roche-lobe overflow and, as in the case of close binaries, dynamical mass loss. The gas lost through the cusp goes toward the central body with roughly free-fall velocity. The cusp should be considered, therefore, as the inner edge of the disk. The accretion rate through the cusp $\dot{\mathfrak{M}}_{in}$ and the energy loss rate L_{in} scale as

$$\dot{\mathfrak{M}}_{in} \sim \Sigma_{in} H_{in} \tag{6.1}$$

$$L_{in} \sim \Sigma_{in} H_{in}^3 \ . \tag{6.2}$$

The cusp is located between the marginally bound and marginally stable circular orbit and very close to the sonic point $R = R_s$. For a Schwarzschild black hole it is

$$2\,R_G < R_S < 3\,R_G \ . \tag{6.3}$$

The lower limit corresponds to the location of a circular orbit which is marginally bound in the sense that all the orbits with $R < 2R_G$ are unbound, and all those with $R > 2R_G$ are bound. The upper limit corresponds to the marginally stable circular orbit: orbits with $R < 3R_G$ are unstable and those with $R > 3R_G$ are stable. When $\dot{\mathfrak{M}} \ll \dot{\mathfrak{M}}_c$ the cusp and the sonic point coincide with the marginally stable orbit $R_S < R_{in}\ R_G$, while for $\dot{\mathfrak{M}} \gg \dot{\mathfrak{M}}_c$ the cusp goes very close to the marginally bound orbit. The energy per particle released by the process is the binding energy of the circular orbit located at the cusp. Since this goes to zero at the marginally bound orbit at which the cusp ends for $\dot{\mathfrak{M}} \gg \dot{\mathfrak{M}}_c$, also the efficiency of the process tends to zero. It can be shown, in particular, that the radiated luminosity L grows only logarithmically with the accretion rate for $\dot{\mathfrak{M}} \gg \dot{\mathfrak{M}}_c$. One can therefore conclude that stationary disks with $\dot{\mathfrak{M}} \gg \dot{\mathfrak{M}}_c$ have low efficiency compared to standard disks. However, they have $L > L_E$ for $\dot{\mathfrak{M}} \gg \dot{\mathfrak{M}}_c$.

The thick-disk photosphere emits relatively soft thermal radiation with a spectrum close to a blackbody, characterized by temperatures not very different from the corresponding ones for thin disks. Deep in the funnel at $R = 5\,R_G$ one has

$$T_{max} \sim 10^7 (\dot{\mathfrak{M}}/\dot{\mathfrak{M}}_c)\,(\mathfrak{M}/\mathfrak{M}_\odot)^{-1/4}\ [\mathrm{K}] \tag{6.4}$$

$$h\nu_{max} \sim 1 \times (\dot{\mathfrak{M}}/\dot{\mathfrak{M}}_c)^{1/4}\,(\mathfrak{M}/\mathfrak{M}_\odot)^{-1/4}\ [\mathrm{keV}] \ . \tag{6.5}$$

The interior of the funnel is much hotter than the rest of the disk surface and therefore the same thick disk appears different when observed at different aspect angles.

The stability of thick accretion disks is a subject of very active research at present. Papaloizou and Pringle (1984, 1985) demonstrated that nonaccreting perfect fluid tori orbiting a Newtonian center of gravity are subject to violent global, nonaxially symmetric instability. It is not known at present whether this instability destroys the astrophysically relevant tori (thick disks) because: (1) Frank and Robinson's (1987) numerical models suggest that the importance of this instability decreases with increasing width of the torus. For astrophysically relevant, very big tori, the growth rate of the instability is too slow to be of importance. (2) Blaes (1987) showed that even a modest amount of accretion completely stabilizes the tori; and (3) Goodman and Narayan (1987) demonstrated that self-gravitation also has a stabilizing effect. More theoretical work and sophisticated 3-dimensional hydrodynamical simulations are needed before a final conclusion on the stability of thick disks can be reached.

VII. Accretion and the Realm of Observations

Within the Galaxy, accretion plays a fundamental role in binary systems where the normal star transfers matter to a compact companion. This may happen through a wind or when the normal star overflows the critical equipotential contour connecting the two components of the binary (Roche-lobe overflow). The first instance requires an early-type star, the second a close binary and an evolved companion. Therefore, systems in which the mass transfer occurs through the wind usually contain a massive star and are relatively young, while systems accreting through Roche-lobe overflow are associated with an older stellar population. The accreting object may be a white dwarf, a neutron star, or a black hole. The combination of these possibilities gives rise to a variety of systems carrying information on properties of the collapsed objects (like the spin and the magnetic field), on the astrophysical evolution of the binary, as well as on the physics of the accretion process. Some phenomenological aspects of accreting binaries are illustrated in the following.

An entirely different astrophysical field for which accretion may be relevant is the activity observed in the nuclei of galaxies. The enormous luminosities and the small scales, implied by variability, strongly suggest that the powerhouse is gravitational. However, the connection of the observed phenomena with accretion is still under debate. Some positive indications on the relevance of the accretion process in AGNs will be presented at the end of the chapter.

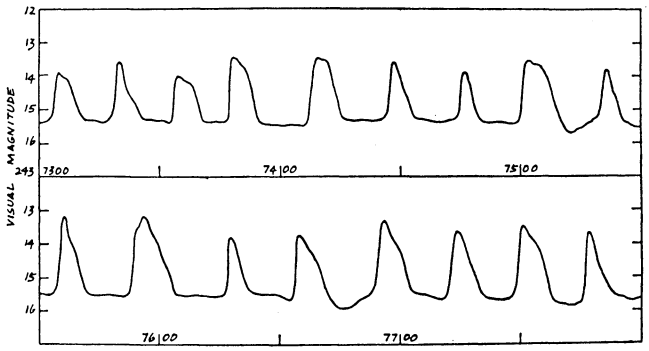

FIG. 10–Light curve of FO Aql (from Glasby 1970).

A. *Cataclysmic Variables*

Cataclysmic variables (CV) are interacting binary systems consisting of a white dwarf (primary) and a late-type star (secondary) transferring mass to the dwarf. The two stars closely orbit each other and the orbital period is always very short: for U Geminorum about four hours. The mass transfer occurs through the Roche lobe, which lies very close to the surface of the secondary.

Direct and detailed observations of disks in cataclysmic variables provide most important data on accretion. From the optical light curves of the eclipsing systems one can infer the contributions of four components: the normal star, an extended accretion disk, a hot spot on the outer rim of the disk, and a bright point source at the disk center. With new techniques of data acquisition and processing, the light distribution in the system can be reconstructed starting from general assumptions.

1. *Dwarf Novae.* One of the basic properties of this subclass of CV is the extreme variability, which is apparent at all wavelengths. In dwarf novae it has the form of recurrent eruptions (see Fig. 10) which may be interpreted as accretion-disk instabilities (e.g., Smak 1984). In these systems the optical (and most probably the total) luminosity of the hot spot is much higher than that of the disk during the quiescence periods. This suggests that during these periods matter is supplied to the outer part of the disk, but only very little actually flows through the disk. From the observation of the changes in luminosity of the dwarf, disk, and hot spot, it was estimated that the amount of matter accreted onto the spot during the quiescence equals the amount accreted onto the dwarf during eruptions. This suggests that matter is gradually accumulated in the outer parts during quiescent periods and accreted onto the dwarf during the eruptions. The eruptions are therefore high-accretion-rate events triggered by an instability in the disk. The recurrence of the eruptions is due to a limit cycle for the disk instability connected with a nonunique dependence of the surface density on the accretion rate, similar to the "S curve" discussed in Section V.F (see also Bath and Pringle 1981, 1983). The calculation of how the limit-cycle behavior at a given radius might translate into a global disk instability propagating over the whole disk structure has been made by several authors (e.g., Meyer and Meyer-Hofmeister 1981; Smak 1984; Papaloizou, Faulkner, and Lin 1983).

Contrary to the case of stationary optically thick disks, where the emitted power and temperature do not depend on the viscosity parameter α, the nonstationary accretion models of dwarf novae strongly depend on α. This gives a unique possibility of an observational evaluation of the viscosity parameter. The typical value needed to fit the observational data to the disk instability models is $\alpha = 0.1$.

It should be noted, however, that in these models α, during the eruptions, is different (higher) than in quiescence. This may follow from the fact that viscosity is due to turbulence connected with a strong convection present during eruptions (Smak 1984).

2. *AM Herculis-Like Objects.* Another especially interesting subclass of cataclysmic variables is represented by AM Her-like objects. These are systems where the white dwarf is endowed with a strong magnetic field $B \sim 10^7$ G. The orbital periods are a few hours, and the separation of the components is smaller than the Alfven radius (eq. (3.7)). In these conditions magnetic torques lock the white-dwarf spin period to the orbital one, and the magnetic field prevents the formation of a disk. The mass transfer occurs directly through a magnetic funnel, where essentially radial inflow is established. As discussed in Section III one expects the formation of a shock, whose temperature is roughly given by equation (3.4). The gas heated at this temperature will emit mainly by bremsstrahlung and cyclotron radiation, because of the strong

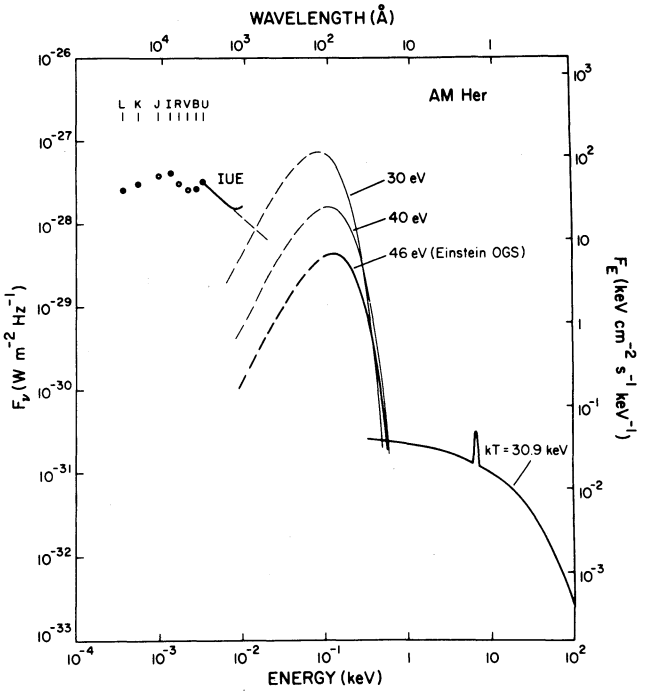

FIG. 11–Spectrum of AM Her (from Lamb 1985).

magnetic field. Part of this energy and of the kinetic energy of the shocked electrons liberated just above the star will be reprocessed at the surface and reemitted as blackbody radiation. The resulting spectrum is rather complicated, since one should take into account the details of radiative transfer. However, in a first approximation one expects three main components, one corresponding to the bremsstrahlung photons at $kT \simeq 10$ keV (eq. (3.2)), one to the cyclotron photons at IR-optical frequencies, and one to blackbody photons at the temperature given by equation (3.1). In Figure 11 we report the observed spectrum of AM Her distinguishing the three components. This agrees in general, but not in detail, with the expectations, in that the blackbody component appears too dominant. For a detailed discussion of the emission of AM Her-like objects we refer, for instance, to Liebert and Stockman (1985) and Lamb (1985).

B. *X-Ray Binaries*

Accreting binary systems containing a neutron star or a black hole are usually, though vaguely, defined as X-ray binaries. The X-ray luminosity (10^{37} erg s^{-1}) is in fact much higher than for cataclysmic variables, due to the fact that the absolute efficiency of accretion reaches the limiting value of 10%. A distribution of the ratio of the X-ray to optical luminosities of identified galactic sources is shown in Figure 12, where the different classes are indicated.

If the neutron star has a high magnetic field ($\sim 10^{12}$ G), the accretion flow is guided through a magnetic funnel (see Section III). The radiative transfer within the funnel is very complex; the emerging radiation is expected to be beamed. The rotation of the neutron star, together with its funnel, gives rise to a periodic modulation of the observed X-ray flux, whence the name of X-ray pulsators. Examples of X-ray light curves are reported in Figure 13, where the modulation with the spin period is apparent. The X-ray spectrum is usually quite hard, and in a few cases cyclotron features around 50 keV corresponding to a field of 10^{12} G have been observed. X-ray pulsators are usually found in systems with a massive young companion. They have orbital periods of order of days and spin periods of order of a second. The mass transfer occurs via a wind.

If the companion of the neutron star is a low-mass (low-luminosity) star, the emission of the system is strongly dominated by the accretion power, which makes it difficult to derive the parameters of the normal star. These systems are old, and the magnetic field is supposedly small (10^9 G), so that it plays a minor role in the dynamics of accretion. The low-mass X-ray binaries (LMXRB) would seem to be ideal systems for the study of accretion disks. However, the actual situation is complicated by the effects on the structure of the accretion disk of the high central X-ray luminosity, released at the boundary of the disk with the neutron star. In particular it has been recognized that above the accretion disk, a corona is present which in some cases may be quite optically thick and reprocess a large fraction of the disk

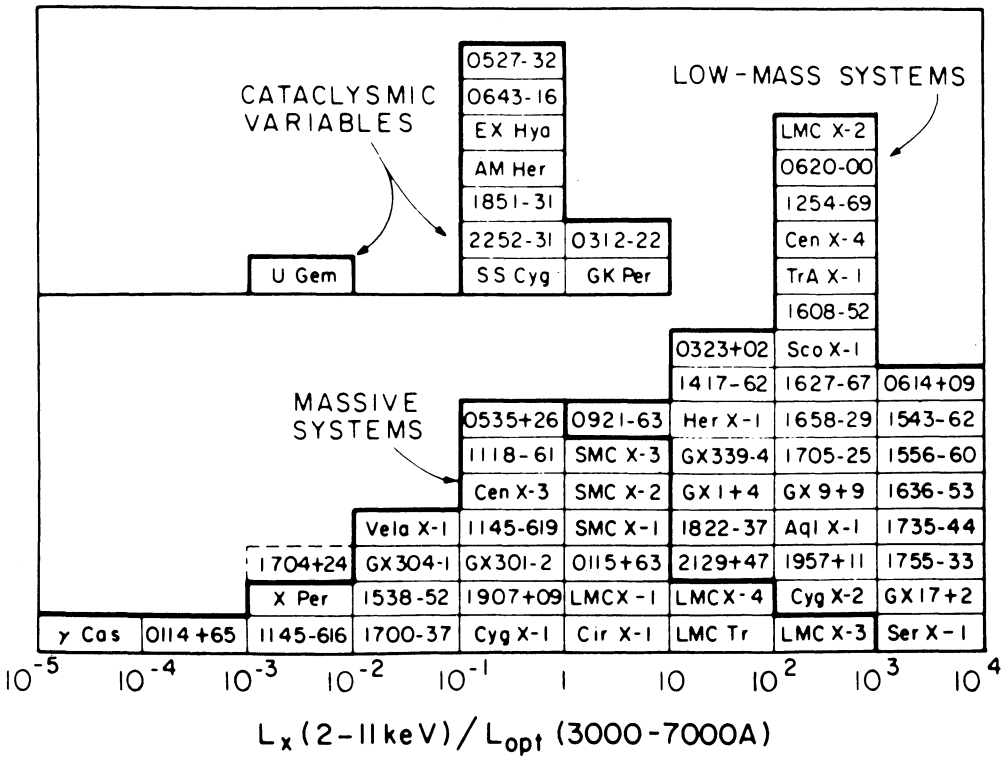

FIG. 12–Distribution of the ratio of X-ray to optical luminosity for binary systems (from Bradt and McClintock 1983).

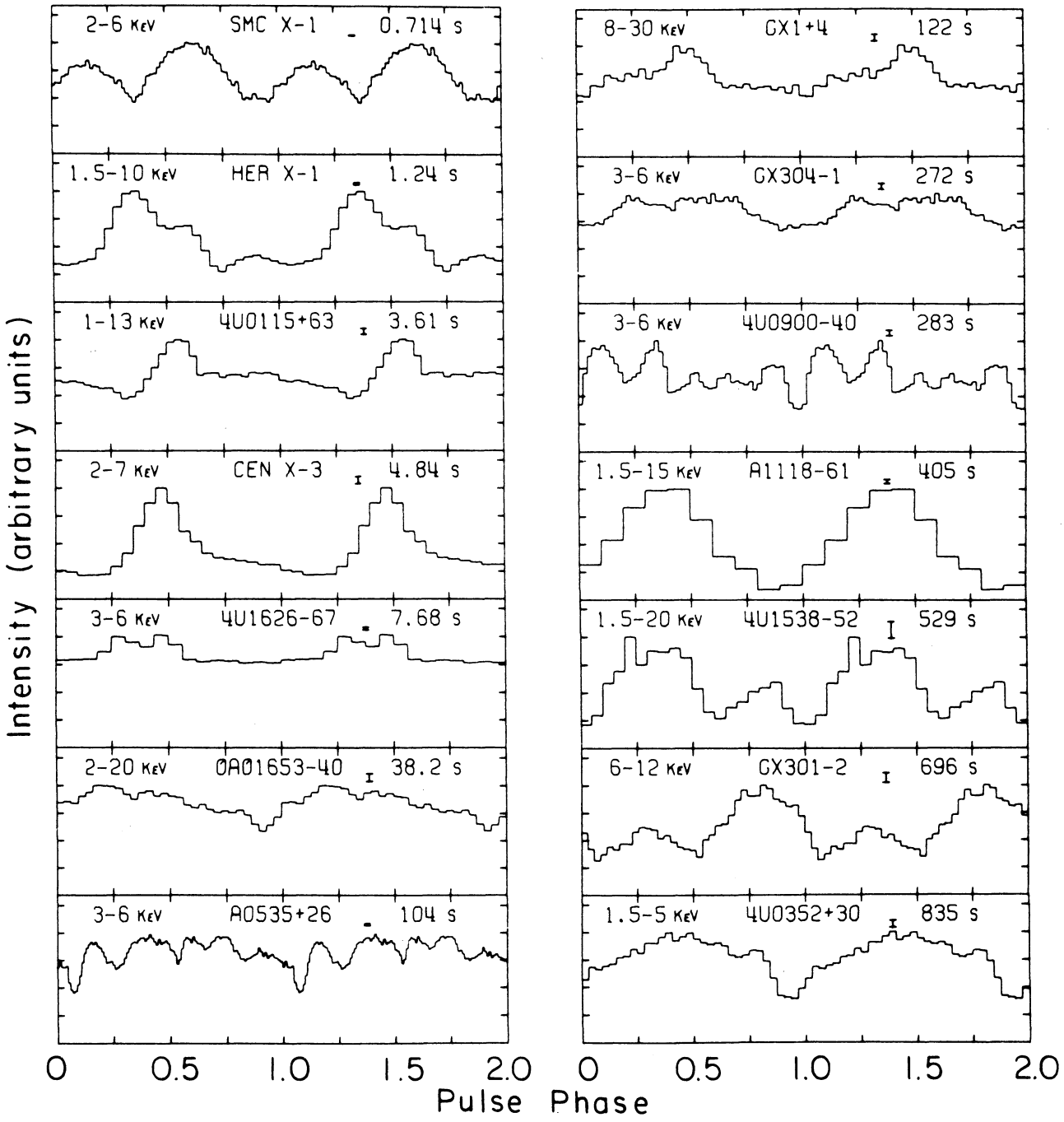

FIG. 13–Pulse profiles of some X-ray pulsators (from Joss and Rappaport 1984).

and boundary-layer luminosity.

X-ray spectra of LMXRB are generally softer than those of pulsators. Spectral models involving the superposition of a blackbody component and a thermal bremsstrahlung can satisfactorily account for the observations (see Fig. 14). While the former component may be directly associated with the neutron-star emission, as indicated by the dimension of the emitting region, the origin of the bremsstrahlung component, and in particular its relation with the emission from the disk or its corona, are still unclear. The fact that the bremsstrahlung component contains the bulk of the luminosity appears as a severe difficulty (e.g., White, Stella, and Parmer 1988). It is possible that the spectral deconvolution used up to now is still inadequate to represent the intrinsic energy distribution.

No strictly periodic component is found in the X-ray emission of most LMXRB, which is taken as evidence of the modestness of the magnetic field. However, recently it was recognized that quasi-periodic short-lived modula-

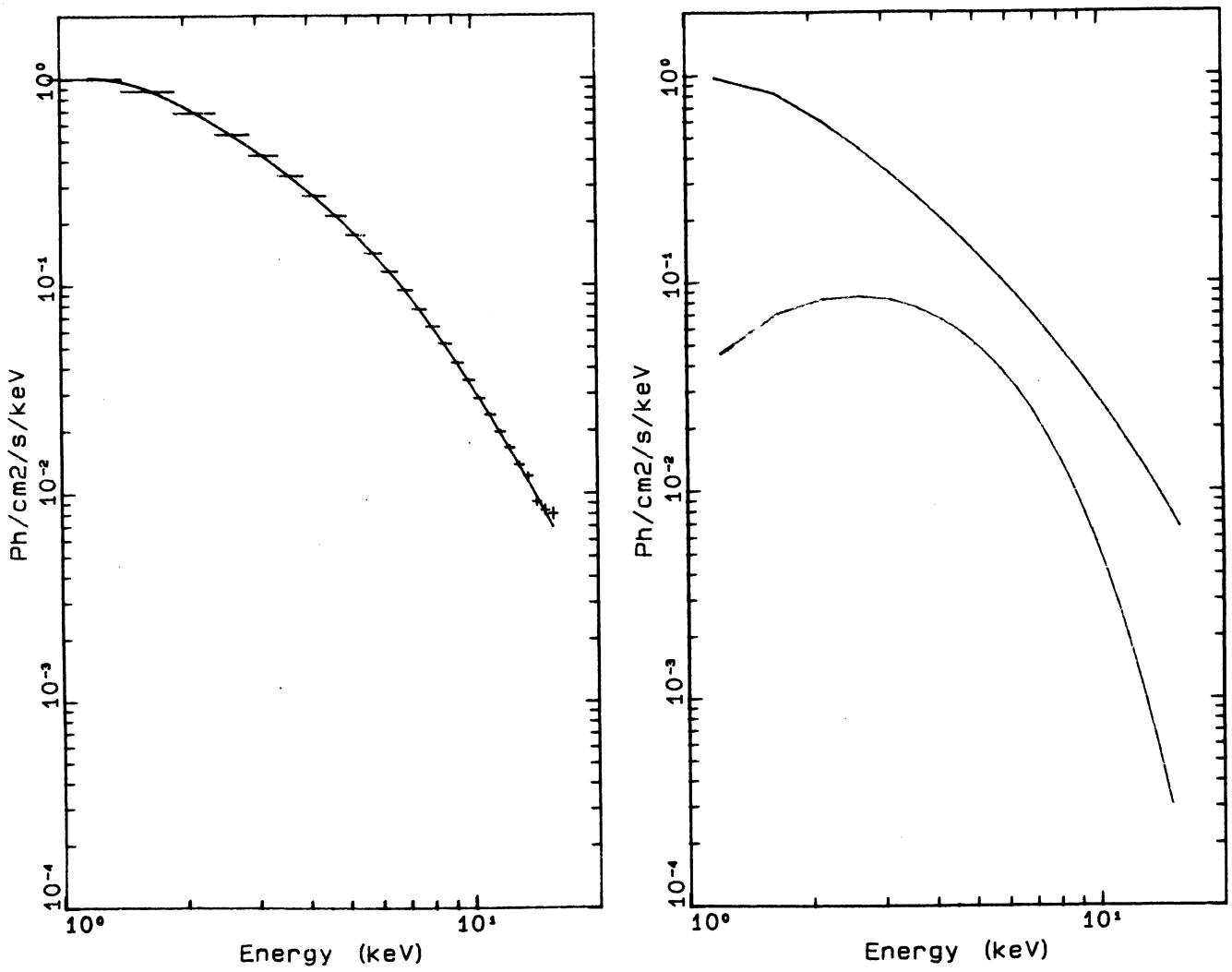

FIG. 14–X-ray spectrum of Cyg X2 and its deconvolution into a blackbody and a thermal bremsstrahlung (TB) component (courtesy of L. Chiappetti).

tion is present in various sources. Examples of power spectra are reported in Figure 15. The origin of quasi-periodic oscillations (QPO) is as yet unclear. There are proposals of a relation to accretion-disk instabilities, or to the interaction of the inner disk with an Alfven surface, with dimensions comparable to the neutron star radius. In any case it appears that QPO will become a prime instrument to gain information on the mode of accretion of LMXRB.

There are three binary X-ray sources which are thought to contain a black hole: Cygnus X-1, LMC X-3, and A 0620-00. The main evidence on the nature of the collapsed object derives from the measurement of the mass function, which yields a mass larger than the upper bound for neutron stars ($\sim 3\,\mathfrak{M}_\odot$). For two of these objects, Cyg X-1 and LMC X-3, good-quality X-ray spectra are available. They are shown in Figure 16. Both are well fitted by models in which the spectra are the product of multi-Compton scattering of a soft photon population in a hot thermal plasma. The process has been briefly described in Section IV. In such a picture the spectrum is determined by the optical depth and temperature. For both objects the derived temperatures are much lower and the optical depths larger than those expected in the proximity of the hole in a spherical model (§ IV). A general and quantitative treatment of the disk spectrum in the Comptonization regime has not been given yet. In any case the optical depths are smaller than would be obtained applying the standard model in a consistent way. In particular, the observed trend of lower optical depth with lower luminosity is opposite to that predicted by the "standard" model.

C. *Active Galactic Nuclei*

Active Galactic Nuclei (AGN) have been the subject of several excellent reviews in recent years (e.g., Begelman, Blandford, and Rees 1984; Lawrence 1987). An enlightening discussion of models of accretion onto massive black

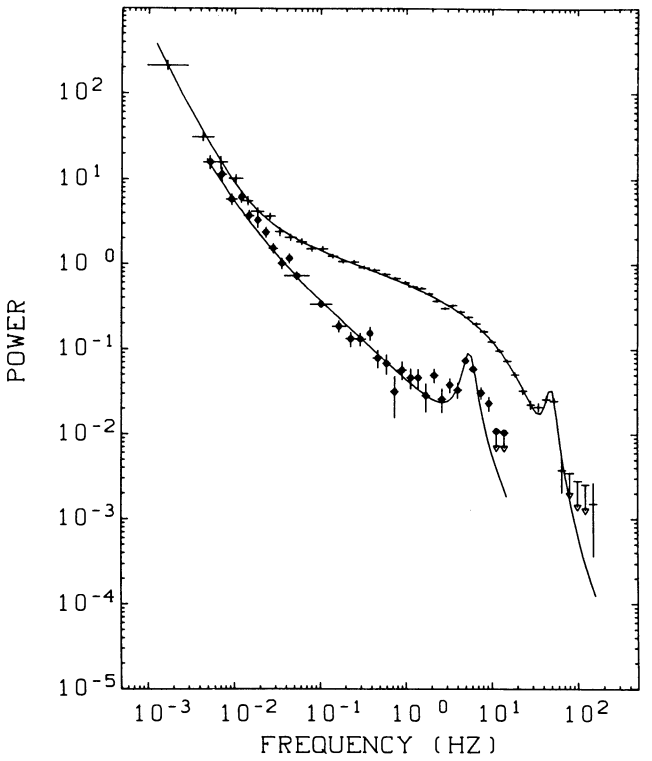

FIG. 15–Power spectrum of sources exhibiting quasi-periodic oscillations of Cyg X2 (from Hasinger 1988).

holes in relation to AGNs was given by Rees (1984). It is beyond the scope of this paper to give an overview of various possible schemes, since the activity of galactic nuclei involves many types of disparate phenomena which are interrelated. We merely wish to stress here two aspects. The first concerns the broad-band energy distribution and the second the variability of AGNs.

The continuum emitted by AGNs extends, in most cases, from the far infrared to the X-rays. This is probably due to the contribution of several components, which are not easy to distinguish on the basis of narrow-band spectra alone. Only recently, broad-band energy distributions have been determined for a large number of objects (e.g., Edelson and Malkan 1986). From this work it clearly appears that the optical-ultraviolet continuum of most quasars and Seyfert galaxies is characterized by a flat shape, energy spectral index 0.5, at variance with the overall energy distribution, which is generally steeper. This excess, which is generally referred to as the "3000 Å bump" (see Fig. 17) is such as to imply that most of the power is emitted in the far-ultraviolet band and is strongly suggestive of a thermal process, although information on the shape of the peak is still scarce (Edelson and Malkan 1986). The idea that the bump may be due to optically-thick emission from an accretion disk, originally proposed by Shields (1978) and Malkan and Sargent (1982), encounters increasing consensus, although detailed spectral modeling has only recently begun (e.g., Czerny and Elvis 1987; Madau 1988; Malkan and Sun 1988). This spectral component appears as the most promising link between AGNs and accretion models, and we expect that this area will see a major development over the next few years.

A second crucial issue is that of time variability. Many Seyfert galaxies and a few quasars have been observed to be variable in X-rays on time scales of hours. The data do not allow us to define unambiguously the characteristic time scale; nevertheless, it is interesting to evaluate the maximum observed luminosity variation and compare with the predictions of models. Since it is difficult to exceed the Eddington luminosity (see Section IV), the larger the luminosity, the larger should be the mass of the central black hole. Assuming that the minimum time scale of variability is related to the size of the gravitational radius of the black hole, one expects that the larger the luminosity is the longer the variability time scale becomes. It is interesting that the data, though still somewhat confused, show indeed some correlation of the time scale with the luminosity (see Fig. 18).

In particular, the present data seem to be in agreement with the expectations of the accretion models in the case of the X-ray emission of Seyfert galaxies and low-luminosity quasars, but not for BL Lacertae objects which could represent a different class of AGNs.

It would be a major step forward in our knowledge of AGNs if X-ray astronomy in the near future should provide a statistically firm basis for this claim.

VIII. Conclusions

The formidable observational advances in the last two decades have assured a fundamental role to accretion theory in today's astrophysics. A comparison can be made, perhaps, with the theory of energy production by nuclear processes, which was one of the triumphs of astrophysics in the thirties. At present the basic frame of accretion theory seems well established, with the theory entering into a phase of maturity. The principal problem is now a direct connection of the theory with observations. The main difference with respect to stellar interiors is that, due to the very different opacity and time scale involved, the former are extremely steady while, in the case of accretion, variability plays a major role. One can hope to reconstruct the dynamics from the study of variability. Furthermore, one of the fascinating aspects of the accretion process is that the region of maximum energy production may in some cases be directly observable.

Substantially new input will derive in the near future from spectral and variability observations, especially at UV and X-ray frequencies. Progress in the theory is expected from numerical work for constructing more realistic models along the lines that we have tried to expose in the previous sections and, hopefully, from radically new approaches.

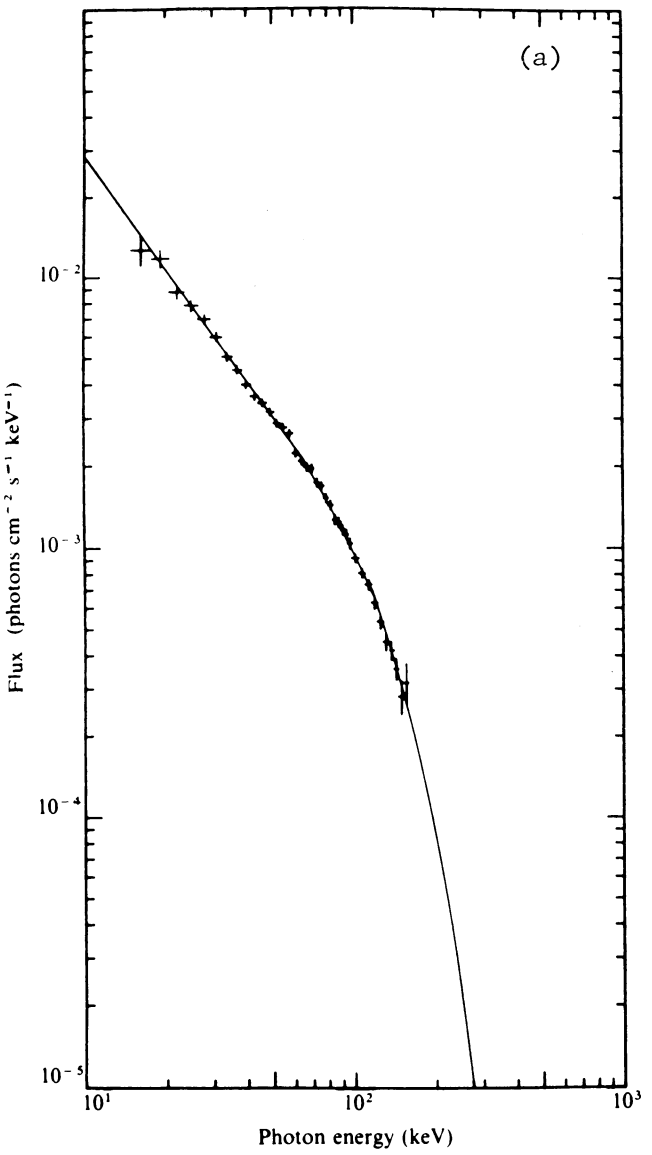

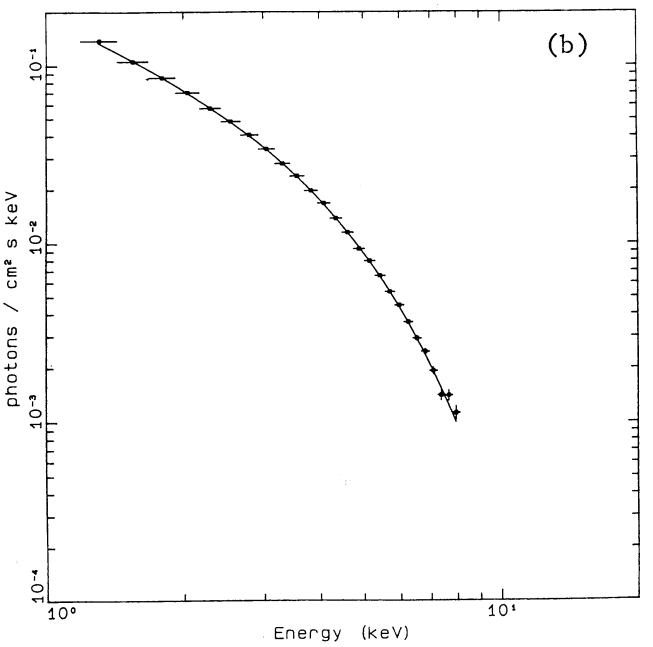

FIG. 16–X-ray spectra of two black hole candidates: Cyg X1 (a) and LMC X3 (b) (from Sunyaev and Truemper 1979 and Treves *et al.* 1988).

We are grateful to M. Colpi, A. Lightman, and J. Miller for a careful reading of the paper.

REFERENCES

Abramowicz, M. A., and Marsi, C. 1987, *Observatory*, **107**, 245.
Abramowicz, M. A., Calvani, M., and Nobili, L. 1980, *Ap. J.*, **242**, 772.
Abramowicz, M. A., Czerny, B., Lasota, J. P., and Szuszkiewicz, E. 1988, *Ap. J.*, in press.
Aizu, K. 1973, *Progr. Theor. Phys.*, **49**, 1184.
Alme, M. L., and Wilson, J. R. 1973, *Ap. J.*, **186**, 1015.
Baan, W. A., and Treves, A. 1973, *Astr. Ap.*, **22**, 421.
Barr, P. 1986, in *The Physics of Accretion onto Compact Objects*, ed. K. O. Mason, M. G. Watson, and N. E. White (Berlin: Springer).
Bath, G. T., and Pringle, J. E. 1981, *M.N.R.A.S.*, **194**, 967.
———. 1983, *M.N.R.A.S.*, **199**, 267.
Begelman, M. C. 1978, *M.N.R.A.S.*, **184**, 53.
———. 1979, *M.N.R.A.S.*, **187**, 237.
Begelman, M. C., and Chiueh, T. 1987, preprint.
Begelman, M. C., Blanford, R. D., and Rees, M. J. 1984, *Rev. Mod. Phys.*, **56**, 225.
Bisnovatyi-Kogan, G. S. 1979, *Riv. Nuovo Cimento*, **2**, 1.
Blaes, O. M. 1987, *M.N.R.A.S.*, **227**, 975.
Bondi, H. 1952, *M.N.R.A.S.*, **112**, 195.
Bradt, H. V., and McClintock, J. E. 1983, *Ann. Rev. Astr. Ap.*, **21**, 13.
Colpi, M. 1988, *Ap. J.*, **226**, 223.
Colpi, M., Maraschi, L., and Treves, A. 1984, *Ap. J.*, **280**, 319.
———. 1986, *Ap. J.*, **311**, 150.
Cowie, L. L., Ostriker, J. P., and Stark, A. A. 1978, *Ap. J.*, **226**, 1041.
Czerny, B., and Elvis, M. 1987, *Ap. J.*, **321**, 305.
Davidson, K., and Ostriker, J. P. 1973, *Ap. J.*, **179**, 585.
Edelson, P. A., and Malkan, M. A. 1986, *Ap. J.*, **308**, 59.
Elvis, M., Czerny, B., and Wilkes, B. J. 1986, in *The Physics of Accretion onto Compact Objects*, ed. K. O. Mason, M. G. Watson, and N. E. White (Berlin: Springer).
Fabian, A. C., Pringle, J. A., and Rees, M. J. 1976, *M.N.R.A.S.*, **175**, 43.
Flammang, R. A. 1982, *M.N.R.A.S.*, **199**, 833.
———. 1984, *M.N.R.A.S.*, **206**, 589.
Frank, J., and Robinson, J. 1987, preprint.
Frank, J., King, A. R., and Raine, D. J. 1985, *Accretion Power in Astrophysics* (Cambridge: Cambridge University Press).
Glasby, J. S. 1970, *The Dwarf Novae* (London: Constable and Co.).
Goodman, J., and Narayan, R. 1987, preprint.
Hasinger, G. 1988, *Astr. Ap.*, in press.
Holzer, T. E., and Axford, W. I. 1970, *Ann. Rev. Astr. Ap.*, **8**, 31.
Hoshi, R. 1973, *Progr. Theor. Phys.*, **49**, 776.
Hoyle, F., and Lyttleton, R. A. 1939, *Proc. Cam. Phil. Soc.*, **35**, 405.
Ipser, J. R., and Price, R. H. 1977, *Ap. J.*, **216**, 578.
———. 1982, *Ap. J.*, **255**, 654.
———. 1983, *Ap. J.*, **267**, 371.
Jaroszynski, M., Abramowicz, M. A., and Paczynski, B. 1980, *Acta. Astr.*, **30**, 1.
Joss, P. C., and Rappaport, S. A. 1984, *Ann. Rev. Astr. Ap.*, **22**, 537.
Klein, R. L., Stockman, H. S., and Chevalier, R. A. 1980, *Ap. J.*, **237**, 912.
Lamb, D. Q. 1985, in *Cataclysmic Variables and Low Mass X-Ray*

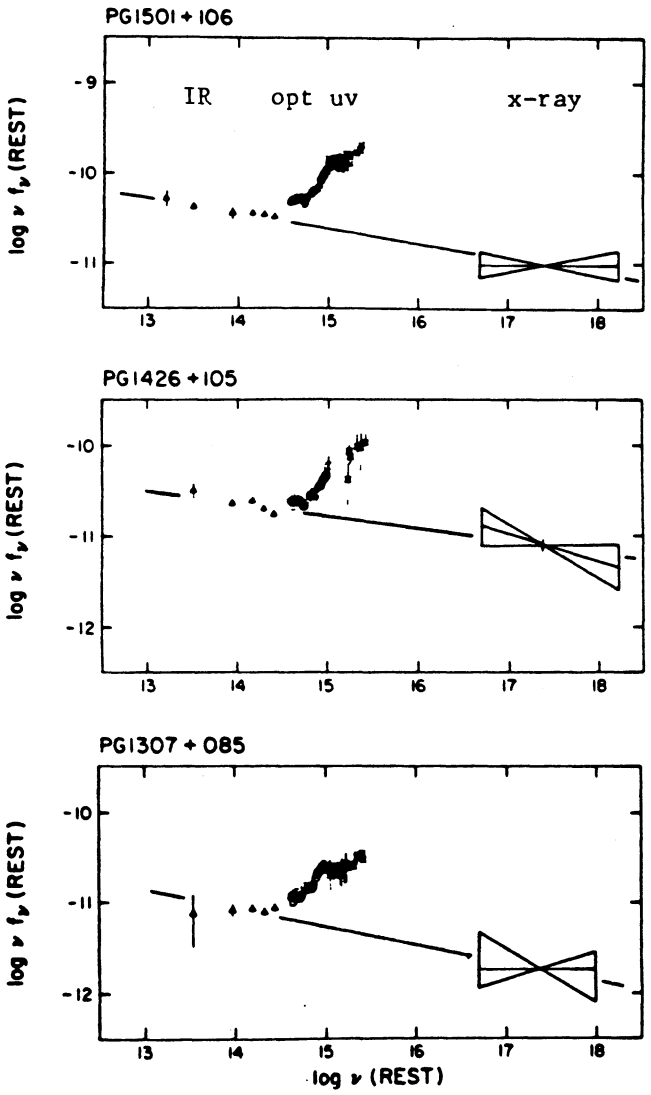

FIG. 17–Examples of blue bumps in quasars (from Elvis *et al.* 1986).

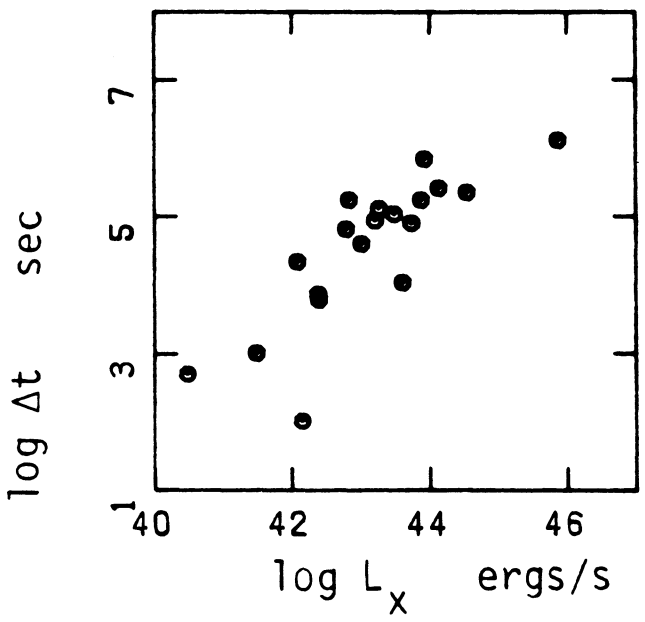

FIG. 18–Variability time scale vs. X-ray luminosity for Active Galactic Nuclei (from Barr 1986).

Binaries, ed. D. Q. Lamb and J. Patterson (Dordrecht: Reidel).
Lamb, F. K., Pethick, C. J., and Pines, D. 1973, *Ap. J.*, **174**, 271.
Landau, L. D., and Lifshitz, E. 1959, *Fluid Mechanics* (New York: Pergamon).
Lawrence, A. 1987, *Pub. A.S.P.*, **99**, 309.
Liebert, J., and Stockman, H. S. 1985, in *Cataclysmic Variables and Low Mass X-Ray Binaries*, ed. D. Q. Lamp and J. Patterson (Dordrecht: Reidel).
Lightman, A. P. 1974, *Ap. J.*, **194**, 429.
Lightman, A. P., and Eardley, D. M., 1974, *Ap. J. (Lettters)*, **187**, L1.
Lightman, A. P., Zdziarski, A. A., and Rees, M. J. 1987, *Ap. J. (Letters)*, **315**, L113.
Lyndell-Bell, D. 1969, *Nature*, **226**, 64.
Madau, P. 1988, *Ap. J.*, **327**, 116.
Malkan, M. A., and Sargent, W. L. 1982, *Ap. J.*, **254**, 22.
Malkan, M. A., and Sun, W. H. 1988, preprint.
Maraschi, L., Perola, G. C., Reina, C., and Treves, A., 1979, *Ap. J.*, **230**, 243.
Maraschi, L., Reina, C., and Treves, A. 1974, *Ap. J.*, **35**, 389.
———. 1978, *Astr. Ap.*, **66**, 99.
Maraschi, L., Roasio, R., and Treves, A. 1982, *Ap. J.*, **253**, 312.
Meszaros, P. 1975, *Astr. Ap.*, **44**, 59.
Meszaros, P., and Nagel, W. 1985*a*, *Ap. J.*, **298**, 147.
———. 1985*b*, *Ap. J.*, **299**, 138.
Meyer, F., and Meyer-Hofmeister, E. 1981, *Astr. Ap.*, **104**, 40.
Novikov, I. D., and Thorne, K. S. 1973, in *Black Holes*, ed. C. DeWitt and B. DeWitt (New York: Gordon and Breach).
Paczynski, B., and Wiita, P. 1980, *Astr. Ap.*, **88**, 23.
Papaloizou, J. C., and Pringle, J. E. 1984, *M.N.R.A.S.*, **208**, 721.
———. 1985, *M.N.R.A.S.*, **213**, 799.
Papaloizou, J., Faulkner, J., and Lin, D. N. 1983, *M.N.R.A.S.*, **205**, 487.
Parker, E. N. 1963, *Interplanetary Dynamical Processes* (New York: Interscience).
Piran, T. 1978, *Ap. J.*, **221**, 652.
Pozdnyakov, L. A., Sobol', I. M., and Sunyaev, R. A. 1983, *Ap. Space Sci. Rev.*, **2**, 189.
Prendergast, K. H., and Burbidge, G. R. 1968, *Ap. J. (Letters)*, **151**, L83.
Pringle, J. E., 1981, *Ann. Rev. Astr. Ap.*, **19**, 137.
Pringle, J. E., and Rees, M. J. 1972, *Astr. Ap.*, **21**, 1.
Pringle, J. E., Rees, M. J., and Pacholczyk, A. G. 1973, *Astr. Ap.*, **29**, 179.
Rees, M. J. 1978, *Phys. Scripta*, **17**, 193.
———. 1984, *Ann. Rev. Astr. Ap.*, **22**, 471.
Rees, M. J., Begelman, M. C., Blandford, R. D., and Phinney, E. S. 1982, *Nature*, **295**, 17.
Rybicki, G. B., and Lightman, A. 1979, *Radiative Processes in Astrophysics* (New York: Wiley).
Salpeter, E. E. 1964, *Ap. J.*, **140**, 796.
Shakura, N. I. 1972, *Astr. Zu.*, **49**, 921.
Shakura, N. I., and Sunyaev, R. A. 1973, *Astr. Ap.*, **24**, 337.
———. 1976, *M.N.R.A.S.*, **175**, 613.
Shapiro, S. L. 1973*a*, *Ap. J.*, **180**, 531.
———. 1973*b*, *Ap. J.*, **185**, 69.
Shapiro, S. L., and Salpeter, E. E. 1975, *Ap. J.*, **198**, 671.

Shapiro, S. L., and Teukolsky, S. A. 1983, *Black Holes, White Dwarfs and Neutron Stars* (New York: Wiley).
Shapiro, S. L., Lightman, A. P., and Eardley, D. M. 1976, *Ap. J.*, **204**, 187.
Shields, G. 1978, *Nature*, **272**, 706.
Shklovsky, I. S. 1967, *Ap. J. (Letters)*, **148**, L1.
Shvartsman, V. F. 1971, *Soviet Astr.*, **15**, 37.
Smak, J. I. 1984, *Pub. A.S.P.*, **96**, 5.
Sunyaev, R. A., and Titarchuk, L. G. 1980, *Astr. Ap.*, **86**, 121
Sunyaev, R. A., and Truemper, J. 1979, *Nature*, **279**, 508.
Takahara, F., Tsuruta, S., and Ichimura, S., 1981, *Ap. J.*, **251**, 26.
Thorne, K. S., Flammang, R. A., and Zytkow, A. N. 1981, *M.N.R.A.S.*, **194**, 475.
Treves, A., Belloni, T., Chiappetti, L., Maraschi, L., Stella, L., Tanzi, E. G., and van der Klis, M. 1988, *Ap. J.*, **325**, 119.
Turolla, R., Nobili, L., and Calvani, M. 1986, *Ap. J.*, **303**, 573.
White, N. E., Stella, L., and Parmar, A. N. 198, *Ap. J.*, **324**, 363.
Zdziarski, A. A. 1985, *Ap. J.*, **289**, 51.
Zel'dovich, Ya. B. 1964, *Soviet Phys. Doklady*, **9**, 195.
Zel'dovich, Ya. B., and Novikov, I. D. 1971, *Relativistic Astrophysics*, Vol. 1 (Chicago: University of Chicago Press).
Zel'dovich, Ya., and Shakura, N. I. 1969, *Soviet Astr.*, **13**, 175.